CONDENSED MATTER PHYSICS

Refined symmetry indicators for topological superconductors in all space groups

Seishiro Ono[1], Hoi Chun Po[2]*, Haruki Watanabe[3]*†

Topological superconductors are exotic phases of matter featuring robust surface states that could be leveraged for topological quantum computation. A useful guiding principle for the search of topological superconductors is to relate the topological invariants with the behavior of the pairing order parameter on the normal-state Fermi surfaces. The existing formulas, however, become inadequate for the prediction of the recently proposed classes of topological crystalline superconductors. In this work, we advance the theory of symmetry indicators for topological (crystalline) superconductors to cover all space groups. Our main result is the exhaustive computation of the indicator groups for superconductors under a variety of symmetry settings. We further illustrate the power of this approach by analyzing fourfold symmetric superconductors with or without inversion symmetry and show that the indicators can diagnose topological superconductors with surface states of different dimensionalities or dictate gaplessness in the bulk excitation spectrum.

INTRODUCTION

Unconventional pairing symmetry in a superconductor indicates a departure from the well-established Bardeen-Cooper-Schrieffer (BCS) paradigm for superconductivity. Such systems, exemplified by the high-temperature superconductors like the cuprate, typically display a wealth of intricate, oftentimes mysterious, phenomena that are of great theoretical, experimental, and technological interest (*1*). The physics of unconventional superconductors has gained a new dimension in the past decade, thanks to the bloom in the understanding of topological quantum materials (*2*–*4*). A hallmark of topological superconductors (TSCs) is the presence of robust surface states that correspond to Majorana fermions—an exotic emergent excitation that can loosely be described as being half of an ordinary electron. These Majorana excitations might be harvested for topological quantum computation, and much effort has been paid to the experimental realization of such exotic phases of matter (*5*).

The intense research effort on topological quantum materials has resulted in an ever increasing arsenal of experimentally verified topological (crystalline) insulators and semimetals, but the discovery of TSCs has proven to be much more challenging. The theoretical landscape, however, has evolved rapidly in recent years. On the one hand, the complex problem of how the diverse set of spatial symmetries in a crystal can both prohibit familiar topological phases and protect new ones has largely been solved, with the theoretical efforts culminating in the production of general classifications for topological crystalline phases in a variety of symmetry settings (*6*–*13*). On the other hand, general theories for how crystalline symmetries can be used to identify topological materials have been developed (*14*, *15*). In particular, the method of symmetry indicators (SIs) (*14*) has enabled comprehensive surveys of topological materials among existing crystal structure databases, and thousands of materials candidates have been uncovered (*16*–*18*).

It is natural to ask if the theory of SIs could be used to facilitate the discovery of TSCs. There are two main difficulties: First, unconventional superconductivity emerges out of strong electronic correlations, and for such systems, theoretical treatments using different approximation schemes rarely converge to the same answers. Such debates could only be settled by meticulous experimental studies, which could take years to be completed. Second, even within the simplifying assumption that a mean-field Bogoliubov–de Gennes (BdG) provides a satisfactory treatment for the system, the original theory of SIs falls short in identifying key examples of TSCs like the one-dimensional (1D) Kitaev chain (*19*–*21*) and its higher-dimensional analogs like the higher-order TSCs in 2D (*22*, *23*). We remark that alternative formulas relating the signs of the pairing order parameters on different Fermi surfaces and topological invariants also exist in the literature, but this approach requires more detailed knowledge on the system than just the symmetry representations (*24*). Furthermore, the extension of these formulas for other crystalline and higher-order TSCs has only been achieved for specific examples (*25*–*27*).

In this work, we address the second part of the problem by extending the theory of SIs to the study of TSCs described by a mean-field BdG Hamiltonian in any space group. This is achieved by a refinement of the SI for TSCs, which was previously proposed in (*20*, *21*) and analyzed explicitly for inversion-symmetric systems. Technically, our results do not rely on the weak pairing assumption, which states that the superconducting gap scale is much smaller than the normal-state bandwidth (*19*, *24*, *28*, *29*). In practice, however, the prediction from this method is most reliable when the assumption is valid. For such weakly paired superconductors, only two pieces of data are required to diagnose a TSC: (i) the normal-state symmetry representations of the filled bands at the high-symmetry momenta and (ii) the pairing symmetry.

Our key result is the exhaustive computation of the refined SI groups for superconductors with or without time-reversal symmetry and spin-orbit coupling, which are tabulated in section S1. In the main text, we will first review the topology of superconductors ("Topology of superconductors" section), followed by the "Refined symmetry indicators for superconductors" section, in which we give an interpretative elaboration for the SI refinement proposed in (*20*, *21*). As an example of the results, we will provide an in-depth discussion on the refined SIs for class DIII systems with C_4 rotation symmetry in the "Interpretation of computed symmetry indicators for

[1]Institute for Solid State Physics, University of Tokyo, Kashiwa 277-8581, Japan. [2]Department of Physics, Massachusetts Institute of Technology, Cambridge, MA 02139, USA. [3]Department of Applied Physics, University of Tokyo, Tokyo 113-8656, Japan.
*These authors contributed equally to this work.
†Corresponding author. Email: haruki.watanabe@ap.t.u-tokyo.ac.jp

superconductors" section, and a summary of the SIs for other key symmetry groups is provided in section S2.

Curiously, we discover that the refined C_4 SI is, like the Fu-Kane parity formula (*30*) and the corresponding version for odd-parity TSC (*28*, *29*), linked to the $\mathbb{Z}_2$ quantum spin Hall (QSH) index in the 10-fold way classification of TSC. This link is established in the "Indicators for Wannierizable topological superconductors" section and is perhaps surprising given the SI refinement captured TSCs with corner modes in systems with inversion symmetry (*20*, *21*). To our knowledge, this also represents the first instance of diagnosing a QSH phase using a proper rotation symmetry. Instead of a reduction in the wave function–based formula for the topological index to the symmetry representations, as was done in the original Fu-Kane approach (*30*), our argument relies on an introduction of a class of phases that we dub "Wannierizable TSCs" (WTSCs). We will conclude and highlight a few future directions in Discussion.

THEORETICAL FRAMEWORK

Topology of superconductors

In this section, we review the framework of describing TSCs by BdG Hamiltonians as a preparation for formulating SIs in the "Refined symmetry-indicators for superconductors" section. Our discussion elucidates the possibility of marginally topological SCs, which may be called fragile TSCs.

Symmetry of BdG Hamiltonian

Let us consider the Hamiltonian $H_{\boldsymbol{k}}$ of the normal phase, which we assume to be a D-dimensional Hermitian matrix. We take a superconducting gap function $\Delta_{\boldsymbol{k}}$ that satisfies $\Delta_{\boldsymbol{k}} = -\xi \Delta_{-\boldsymbol{k}}^T$, which is also a square matrix with the same dimension. The parameter ξ can be either +1 or −1 depending on the physical realization. We then form the $2D$-dimensional BdG Hamiltonian

$$H_{\boldsymbol{k}}^{\mathrm{BdG}} \equiv \begin{pmatrix} H_{\boldsymbol{k}} & \Delta_{\boldsymbol{k}} \\ \Delta_{\boldsymbol{k}}^\dagger & -H_{-\boldsymbol{k}}^* \end{pmatrix} \tag{1}$$

This Hamiltonian always has the particle-hole symmetry

$$\Xi_D H_{\boldsymbol{k}}^{\mathrm{BdG}*} \Xi_D^\dagger = -H_{-\boldsymbol{k}}^{\mathrm{BdG}} \tag{2}$$

$$\Xi_D \equiv \begin{pmatrix} & \xi \mathbb{1}_D \\ +\mathbb{1}_D & \end{pmatrix} \tag{3}$$

Here $\mathbb{1}_D$ stands for the D-dimensional identity matrix. Throughout this work, all blank entries of a matrix should be understood as 0. The particle-hole symmetry in Eq. 3 satisfies $\Xi_D^2 = +\xi$. To see the consequence of the particle-hole symmetry, suppose that $\psi_{\boldsymbol{k}}^{\mathrm{BdG}}$ is an eigenstate of $H_{\boldsymbol{k}}^{\mathrm{BdG}}$ with an eigenvalue $E_{\boldsymbol{k}}$. Then, the particle-hole symmetry implies that $\Xi_D \psi_{\boldsymbol{k}}^{\mathrm{BdG}*}$ is an eigenstate of $H_{-\boldsymbol{k}}^{\mathrm{BdG}}$ with eigenvalue $-E_{\boldsymbol{k}}$. We call the eigenvalue $E_{\boldsymbol{k}}$ the quasiparticle spectrum. The BdG Hamiltonian is gapped when the quasiparticle spectrum has a gap around $E = 0$ for all $\boldsymbol{k}$.

Suppose that the Hamiltonian of the normal phase has a space group symmetry G. Each element $g \in G$ is represented by a unitary matrix $U_{\boldsymbol{k}}(g)$ that satisfies

$$U_{\boldsymbol{k}}(g)\, H_{\boldsymbol{k}}\, U_{\boldsymbol{k}}(g)^\dagger = H_{g\boldsymbol{k}} \tag{4}$$

If the gap function satisfies

$$U_{\boldsymbol{k}}(g)\, \Delta_{\boldsymbol{k}}\, U_{-\boldsymbol{k}}(g)^T = \chi_g \Delta_{g\boldsymbol{k}} \tag{5}$$

the spatial symmetry is encoded in the BdG Hamiltonian as

$$U_{\boldsymbol{k}}^{\mathrm{BdG}}(g)\, H_{\boldsymbol{k}}^{\mathrm{BdG}}\, U_{\boldsymbol{k}}^{\mathrm{BdG}}(g)^\dagger = H_{g\boldsymbol{k}}^{\mathrm{BdG}} \tag{6}$$

$$U_{\boldsymbol{k}}^{\mathrm{BdG}}(g) \equiv \begin{pmatrix} U_{\boldsymbol{k}}(g) & \\ & \chi_g U_{-\boldsymbol{k}}^*(g) \end{pmatrix} \tag{7}$$

$$\Xi_D U_{\boldsymbol{k}}^{\mathrm{BdG}}(g)^* \Xi_D^\dagger = \chi_g^* U_{-\boldsymbol{k}}^{\mathrm{BdG}}(g) \tag{8}$$

The 1D representation χ_g of G defines the symmetry property of the superconducting gap $\Delta_{\boldsymbol{k}}$.

Last, the BdG Hamiltonian has the time-reversal symmetry if there exists $U_{\mathcal{T}}$ such that

$$U_{\mathcal{T}} H_{\boldsymbol{k}}^* U_{\mathcal{T}}^\dagger = H_{-\boldsymbol{k}},\ U_{\mathcal{T}} \Delta_{\boldsymbol{k}}^* U_{\mathcal{T}}^T = \Delta_{-\boldsymbol{k}} \tag{9}$$

The representation χ_g must be either ±1 for all $g \in G$. Then, the representation of the time-reversal symmetry in the BdG Hamiltonian is

$$U_{\mathcal{T}}^{\mathrm{BdG}} H_{\boldsymbol{k}}^{\mathrm{BdG}*} U_{\mathcal{T}}^{\mathrm{BdG}\dagger} = H_{-\boldsymbol{k}}^{\mathrm{BdG}} \tag{10}$$

$$U_{\mathcal{T}}^{\mathrm{BdG}} = \begin{pmatrix} U_{\mathcal{T}} & \\ & U_{\mathcal{T}}^* \end{pmatrix} \tag{11}$$

When $\xi = +1$, which is usually the case for electrons, the BdG Hamiltonians without time-reversal symmetry fall into class D of the 10-fold Altland-Zirnbauer (AZ) symmetry classification. When the time-reversal symmetry is present and satisfies $U_{\mathcal{T}}^{\mathrm{BdG}} U_{\mathcal{T}}^{\mathrm{BdG}*} = +1$, the symmetry class becomes BDI, and when it satisfies $U_{\mathcal{T}}^{\mathrm{BdG}} U_{\mathcal{T}}^{\mathrm{BdG}*} = -1$ instead, the symmetry class is DIII. If we discard the particle-hole symmetry from class D, BDI, and DIII, they respectively reduce to class A, AI, and AII. In the presence of spin SU(2) symmetry for spinful electrons, ξ effectively becomes −1 (*31*, *32*). Then, the system without time-reversal symmetry is class C, and with the time-reversal symmetry $U_{\mathcal{T}}^{\mathrm{BdG}} U_{\mathcal{T}}^{\mathrm{BdG}*} = +1$ is class CI. We can formally consider the case $U_{\mathcal{T}}^{\mathrm{BdG}} U_{\mathcal{T}}^{\mathrm{BdG}*} = -1$, which is classified as class CII, but it may be difficult to be realized in electronic systems. The general discussions of this work apply to all of these symmetry classes with the particle-hole symmetry regardless of $\xi = +1$ or −1.

Stacking of BdG Hamiltonians

To carefully define the trivial SCs, let us introduce the formal stacking of two SCs by the direct sum of two BdG Hamiltonians $H_{\boldsymbol{k}}^{\mathrm{BdG}} \oplus H_{\boldsymbol{k}}^{\mathrm{BdG}'}$, in which $H_{\boldsymbol{k}}$ and $\Delta_{\boldsymbol{k}}$ in Eq. 1 are respectively replaced with

$$\begin{pmatrix} H_{\boldsymbol{k}} & \\ & H'_{\boldsymbol{k}} \end{pmatrix}, \begin{pmatrix} \Delta_{\boldsymbol{k}} & \\ & \Delta'_{\boldsymbol{k}} \end{pmatrix} \tag{12}$$

When the dimension of $H'_{\boldsymbol{k}}$ is D', the stacked BdG Hamiltonian is $2(D + D')$–dimensional and has the particle-hole symmetry $\Xi_{D+D'}$.

We furthermore assume that $H_{\boldsymbol{k}}^{\mathrm{BdG}}$ and $H_{\boldsymbol{k}}^{\mathrm{BdG}'}$ have the same spatial symmetry G. Their representations can be different, but χ_g must be common. We define $U_{\boldsymbol{k}}^{\mathrm{BdG}}(g) \oplus U_{\boldsymbol{k}}^{\mathrm{BdG}}(g)'$ by replacing $U_{\boldsymbol{k}}(g)$ in Eq. 7 with

$$\begin{pmatrix} U_{\boldsymbol{k}}(g) & \\ & U_{\boldsymbol{k}}(g)' \end{pmatrix} \tag{13}$$

The possible time-reversal symmetry of the stacked SC is defined in the same way.

Trivial superconductors

Let us now define the topologically trivial class of SCs. Our discussion is inspired by the recent proposal in (*20*, *21*).

Suppose that the BdG Hamiltonian $H_{\boldsymbol{k}}^{\mathrm{BdG}}$ is gapped. We say $H_{\boldsymbol{k}}^{\mathrm{BdG}}$ is strictly trivial when it can be smoothly deformed to either

$$H^{\mathrm{vac}} \equiv \begin{pmatrix} +\mathbb{1}_D & \\ & -\mathbb{1}_D \end{pmatrix} \tag{14}$$

which describes the vacuum state where all electronic levels are unoccupied, or

$$H^{\mathrm{full}} \equiv \begin{pmatrix} -\mathbb{1}_D & \\ & +\mathbb{1}_D \end{pmatrix} \tag{15}$$

which represents the fully occupied state. They are physically equivalent to the chemical potential $\mu = \pm\infty$ limit of $H_{\boldsymbol{k}}^{\mathrm{BdG}}$. Here, the smooth deformation is defined by an interpolating BdG Hamiltonian $H_{\boldsymbol{k}}^{\mathrm{BdG}}(t)$ with

$$H_{\boldsymbol{k}}^{\mathrm{BdG}}(0) = H_{\boldsymbol{k}}^{\mathrm{BdG}},\ H_{\boldsymbol{k}}^{\mathrm{BdG}}(1) = H^{\mathrm{vac}} \text{ or } H^{\mathrm{full}} \tag{16}$$

that maintains both the gap in the quasiparticle spectrum and all the assumed symmetries for all $t \in [0,1]$. Note that we do not modify the representations, such as Ξ_D, $U_{\boldsymbol{k}}^{\mathrm{BdG}}(g)$, and $U_{\mathcal{T}}^{\mathrm{BdG}}$, of assumed symmetries during the process. When a smooth deformation to H^{vac} exists, we write

$$H_{\boldsymbol{k}}^{\mathrm{BdG}} \sim H^{\mathrm{vac}} \tag{17}$$

Similarly

$$H_{\boldsymbol{k}}^{\mathrm{BdG}} \sim H^{\mathrm{full}} \tag{18}$$

when there is an adiabatic path to H^{full}. Under a space group symmetry, conditions Eqs. 17 and 18 are generally inequivalent. The SC is strictly trivial when at least one of the two conditions are fulfilled. For example, the BCS superconductor with SU(2) symmetry, described by

$$H_k^{\mathrm{BdG}} = \begin{pmatrix} -\cos k & \Delta \\ \Delta & \cos k \end{pmatrix} \tag{19}$$

is strictly trivial. This can be seen by the interpolating Hamiltonian

$$H_k^{\mathrm{BdG}}(t) = \cos\left(\frac{\pi t}{2}\right) H_k^{\mathrm{BdG}} \pm \sin\left(\frac{\pi t}{2}\right) H^{\mathrm{vac}} \tag{20}$$

The above definition of trivial SCs is, however, sometimes too restrictive, especially under a spatial symmetry. One instead has to allow for adding trivial degrees of freedom (DOFs). Using the notation summarized in the "Stacking of BdG Hamiltonians" section, we ask if

$$\begin{aligned} &H_{\boldsymbol{k}}^{\mathrm{BdG}} \oplus \begin{pmatrix} -\mathbb{1}_{D'} & \\ & +\mathbb{1}_{D'} \end{pmatrix} \oplus \begin{pmatrix} +\mathbb{1}_{D''} & \\ & -\mathbb{1}_{D''} \end{pmatrix} \\ &\sim H^{\mathrm{vac}} \oplus \begin{pmatrix} +\mathbb{1}_{D'} & \\ & -\mathbb{1}_{D'} \end{pmatrix} \oplus \begin{pmatrix} +\mathbb{1}_{D''} & \\ & -\mathbb{1}_{D''} \end{pmatrix} \end{aligned} \tag{21}$$

See Fig. 1 for the illustration. The right-hand side of this equation is the same as Eq. 14, but the identity matrix is enlarged to $+\mathbb{1}_{D+D'+D''}$. We leverage the freedom in the choice of the matrix size D', D'' and the symmetry representation $U_{\boldsymbol{k}}^{\mathrm{BdG}}(g)'$, $U_{\boldsymbol{k}}^{\mathrm{BdG}}(g)''$ of the trivial DOFs. If, however, there does not exist any smooth path in Eq. 21 for whatever choice of trivial DOFs, then we say $H_{\boldsymbol{k}}^{\mathrm{BdG}}$ is stably topological. It might look unnatural to assign the flipped signs of $\mathbb{1}_{D'}$ between the left- and right-hand side of Eq. 21, but this choice is, in fact, necessary in the presence of space group symmetry in general. This point will become clear in the "Symmetry obstructions" section. Although Eq. 21 describes a smooth deformation to the vacuum state, one can equally consider a deformation to the fully occupied state, which is mathematically equivalent to Eq. 21 as long as trivial DOFs are freely chosen.

These definitions of "strictly trivial SCs" and "stably topological SCs" leave a possibility of fragile topological phases (*33*, *34*), which becomes trivial if and only if appropriate trivial DOFs are added. We will discuss examples of these cases in the "Examples" section.

Examples

As an example of what we explained so far, let us discuss the odd-parity SC in the Kitaev chain (*35*).

Class D. The BdG Hamiltonian of a single Kitaev chain is given by Eq. **1** with

$$H_k = -\cos k,\ \Delta_k = i\sin k \tag{22}$$

This model falls into the $\mathbb{Z}_2$ nontrivial phase in class D and is stably topological.

Let us take two copies of this model by setting

$$H_k = -\cos k\, \mathbb{1}_2,\ \Delta_k = i\sin k\, \mathbb{1}_2 \tag{23}$$

For the doubled BdG Hamiltonian, there exists an adiabatic path for both Eqs. 17 and 18 given by the interpolating Hamiltonian

$$\begin{aligned} H_k^{\mathrm{BdG}}(t) = &\cos\left(\frac{\pi t}{2}\right) H_k^{\mathrm{BdG}} \pm \sin\left(\frac{\pi t}{2}\right) H^{\mathrm{vac}} \\ &+\sin(\pi t) \begin{pmatrix} & & & -i \\ & & i & \\ & -i & & \\ i & & & \end{pmatrix} \end{aligned} \tag{24}$$

which preserves the particle-hole symmetry and the gap in the quasiparticle spectrum. Therefore, the two copies of the Kitaev chain is strictly trivial.

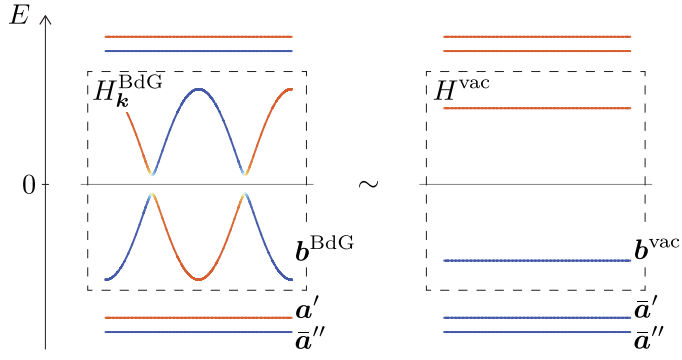

Fig. 1. Illustration of the equivalence relation in Eq. 21. Electron-like states are colored in red, and hole-like states are colored in blue. States outside of the dashed box represent trivial DOFs included in the deformation process. See the "Refined symmetry indicators for superconductors" section for the definition of vectors in this figure.

Class D with inversion symmetry. Let us now take into account the inversion symmetry of the Kitaev chain. For the doubled model, the representation of the inversion symmetry is given by Eq. 7 with

$$U_k(I) = \mathbb{1}_2, \chi_I = -1 \tag{25}$$

where $\chi_I = -1$ indicates odd-parity pairing. Under the inversion symmetry, the adiabatic path in the sense of Eq. 17 or Eq. 18 no longer exists even for the doubled Kitaev model. This can be easily seen by looking at the inversion parity of the quasiparticle spectrum below $E < 0$. On the one hand, in the initial BdG Hamiltonian specified by Eq. 23, the inversion parity of two $E < 0$ levels is both +1 at $k = 0$ and −1 at $k = \pi$. (The opposite parity at $k = 0$ and π is a consequence of $\chi_I = -1$.) On the other hand, in the final trivial Hamiltonian H^{vac} with $D = 2$, the inversion parities of $E = -1$ levels are all −1. If we use H^{full} instead as the trivial Hamiltonian, the inversion parities are all +1. This mismatch of inversion parities serves as an obstruction for any inversion-symmetric adiabatic deformation. The path in Eq. 24 breaks the inversion symmetry for $t \in (0,1)$.

To resolve the obstruction, we introduce trivial DOFs with an appropriate inversion property. Specifically, we set $D' = 2$, $D'' = 0$ and

$$U_k(I)' = \begin{pmatrix} -1 & \\ & -e^{\mathrm{ik}} \end{pmatrix} \tag{26}$$

Now, the inversion parities of $E < 0$ levels on both sides of Eq. 21 agree: two +1's and two −1's at $k = 0$ and one +1 and three −1's at $k = \pi$. There exists an interpolating Hamiltonian

$$\begin{aligned} H_k^{\mathrm{BdG}}(t) &= \cos\left(\frac{\pi t}{2}\right) H_k^{\mathrm{BdG}} \oplus \begin{pmatrix} -\mathbb{1}_2 & \\ & +\mathbb{1}_2 \end{pmatrix} \\ &+ \sin\left(\frac{\pi t}{2}\right) \begin{pmatrix} +\mathbb{1}_4 & \\ & -\mathbb{1}_4 \end{pmatrix} + \sin(\pi t) \begin{pmatrix} \widetilde{\Delta}_k & \\ \widetilde{\Delta}_k^\dagger & \end{pmatrix} \end{aligned} \tag{27}$$

$$\widetilde{\Delta}_k \equiv i \begin{pmatrix} 0 & 0 & 0 & 1+e^{\mathrm{ik}} \\ 0 & 0 & 1 & 0 \\ 0 & -1 & 0 & 1-e^{\mathrm{ik}} \\ -1-e^{-\mathrm{ik}} & 0 & -1+e^{-\mathrm{ik}} & 0 \end{pmatrix} \tag{28}$$

This confirms that the two copies of Kitaev chains with inversion symmetry becomes trivial if and only if proper trivial DOFs are added.

Refined symmetry indicators for superconductors

In this section, we discuss the formalism of SIs for SCs. Our goal is to systematically diagnose the topological properties of SCs described by BdG Hamiltonians using their space group representation. We also clarify the difference between the present approach extending the idea of (*21*, *22*) and the previous approach in (*19*, *36*).

Symmetry representations of BdG Hamiltonians

Let us consider a BdG Hamiltonian $H_{\boldsymbol{k}}^{\mathrm{BdG}}$ in Eq. 1 with a space group symmetry G represented by $U_{\boldsymbol{k}}^{\mathrm{BdG}}(g)$ in Eq. 7. We assume that the spectrum of $H_{\boldsymbol{k}}^{\mathrm{BdG}}$ is gapped at the momentum $\boldsymbol{k}$ for which we study its symmetry properties. Nevertheless, as we explain later, our framework can also be used to diagnose nodal SCs.

Suppose that $\psi_{\boldsymbol{k}}^{\mathrm{BdG}}$ is an eigenstate of $H_{\boldsymbol{k}}^{\mathrm{BdG}}$ and belongs to an irreducible representation $u_{\boldsymbol{k}}^{\alpha}$ of the little group $G_{\boldsymbol{k}} \leq G$ of $\boldsymbol{k}$ (α labels distinct irreducible representations). Then, the particle-hole symmetry implies that $\Xi_D \psi_{\boldsymbol{k}}^{\mathrm{BdG}*}$ belongs to an irreducible representation $\chi_g (u_{\boldsymbol{k}}^{\alpha})^*$ of $G_{-\boldsymbol{k}}$, which can be seen in Eq. 8. We write this correspondence among irreducible representations as

$$u_{\boldsymbol{k}}^{\bar{\alpha}} \equiv \chi_g (u_{-\boldsymbol{k}}^{\alpha})^* \tag{29}$$

The SI is formulated in terms of integers $(n_{\boldsymbol{k}}^{\alpha})^{\mathrm{BdG}}$ that count the number of irreducible representations $u_{\boldsymbol{k}}^{\alpha}(g)$ of $G_{\boldsymbol{k}}$ appearing in the $E < 0$ quasiparticle spectrum. That is, the little group representation formed by all the eigenstates with $E < 0$ can be decomposed into irreducible representations as

$$\oplus_\alpha (n_{\boldsymbol{k}}^{\alpha})^{\mathrm{BdG}} u_{\boldsymbol{k}}^{\alpha}(g) \tag{30}$$

We say $\boldsymbol{k}$ is a high-symmetry point if every point in a neighborhood of $\boldsymbol{k}$ has a lower symmetry than $\boldsymbol{k}$ (*37*). Similarly, $\boldsymbol{k}$ is a point belonging to a high-symmetry line (plane) if a neighborhood of $\boldsymbol{k}$ contains a line (plane) that has the same symmetry as $\boldsymbol{k}$. The set of high-symmetry momenta K contains every high-symmetry point and a representative point from each of the high-symmetry lines and planes. Integers $(n_{\boldsymbol{k}}^{\alpha})^{\mathrm{BdG}}$ are not all independent as they obey compatibility relations as explained in (*12*, *14*, *15*). We compute $(n_{\boldsymbol{k}}^{\alpha})^{\mathrm{BdG}}$ for all α and $\boldsymbol{k} \in K$ and form a vector $\boldsymbol{b}^{\mathrm{BdG}}$, whose components are given by $(n_{\boldsymbol{k}}^{\alpha})^{\mathrm{BdG}}$.

For a later purpose, let us also define $(\bar{n}_{\boldsymbol{k}}^{\alpha})^{\mathrm{BdG}}$ and $\bar{\boldsymbol{b}}^{\mathrm{BdG}}$ using the $E > 0$ quasiparticle spectrum in the same way. Because of the particle-hole symmetry, we find

$$(\bar{n}_{\boldsymbol{k}}^{\alpha})^{\mathrm{BdG}} = (n_{-\boldsymbol{k}}^{\bar{\alpha}})^{\mathrm{BdG}} \tag{31}$$

Next, let us examine a trivial BdG Hamiltonian H^{vac} in Eq. 14 for which the space group G is represented by the same matrix $U_{\boldsymbol{k}}^{\mathrm{BdG}}(g)$ in Eq. 7 as for $H_{\boldsymbol{k}}^{\mathrm{BdG}}$. Observe that $E > 0$ levels of H^{vac} use $U_{\boldsymbol{k}}(g)$ as the representation of $G_{\boldsymbol{k}}$ for every $\boldsymbol{k} \in K$. Similarly, $E < 0$ levels of H^{vac} use $\chi_g U_{-\boldsymbol{k}}(g)^*$ as the representation of $G_{\boldsymbol{k}}$. We define the integers $(\bar{n}_{\boldsymbol{k}}^{\alpha})^{\mathrm{vac}}$ and $(n_{\boldsymbol{k}}^{\alpha})^{\mathrm{vac}}$ by the irreducible decomposition

$$U_{\boldsymbol{k}}(g) = \oplus_\alpha (\bar{n}_{\boldsymbol{k}}^{\boldsymbol{\alpha}})^{\mathrm{vac}} u_{\boldsymbol{k}}^{\alpha}(g) \tag{32}$$

$$\chi_g U_{-\boldsymbol{k}}(g)^* = \oplus_\alpha (n_{\boldsymbol{k}}^{\alpha})^{\mathrm{vac}} u_{\boldsymbol{k}}^{\alpha}(g) \tag{33}$$

and construct vectors $\bar{\boldsymbol{b}}^{\mathrm{vac}}$ and $\boldsymbol{b}^{\mathrm{vac}}$, respectively, using integers $(\bar{n}_{\boldsymbol{k}}^{\alpha})^{\mathrm{vac}}$ and $(n_{\boldsymbol{k}}^{\alpha})^{\mathrm{vac}}$. By construction, we have

$$\boldsymbol{b}^{\mathrm{BdG}} + \bar{\boldsymbol{b}}^{\mathrm{BdG}} = \boldsymbol{b}^{\mathrm{vac}} + \bar{\boldsymbol{b}}^{\mathrm{vac}} \tag{34}$$

since both sides of this equation denote the total representation counts in $U_{\boldsymbol{k}}^{\mathrm{BdG}}(g)$.

Last, we consider additional trivial DOFs described by

$$H^{\mathrm{full}'} \equiv \begin{pmatrix} -\mathbb{1}_{D'} & \\ & +\mathbb{1}_{D'} \end{pmatrix} \tag{35}$$

Suppose that the space group G is represented by $U_{\boldsymbol{k}}^{\mathrm{BdG}}(g)'$ in $H^{\mathrm{full}\prime}$.

We can perform the irreducible decomposition as in Eqs. 32 and 33 and define $\boldsymbol{a}'$ and $\bar{\boldsymbol{a}}'$ using the coefficients for $U_{\boldsymbol{k}}(g)'$ and $\chi_g U_{-\boldsymbol{k}}(g)'^*$, respectively.

Symmetry obstructions

Now, we are ready to derive several obstructions for the smooth deformation in Eqs. 17, 18, and 25. A necessary (but not generally sufficient) condition for the existence of adiabatic paths in Eqs. 17 and 18 is, respectively,

$$\boldsymbol{b}^{\mathrm{BdG}} = \boldsymbol{b}^{\mathrm{vac}} \tag{36}$$

$$\boldsymbol{b}^{\mathrm{BdG}} = \bar{\boldsymbol{b}}^{\mathrm{vac}} \tag{37}$$

When both of these conditions are violated, the representation counts in the $E < 0$ spectrum of the initial and final BdG Hamiltonian in the deformation process do not agree and a smooth symmetric deformation is prohibited. We have seen this already in the doubled Kitaev model with inversion symmetry in the "Examples" section.

Similarly, comparing the representation counts in the $E < 0$ spectrum of the two ends of the adiabatic path of Eq. 21, we find the condition (see Fig. 1)

$$\boldsymbol{b}^{\mathrm{BdG}} + \boldsymbol{a}' + \bar{\boldsymbol{a}}'' = \boldsymbol{b}^{\mathrm{vac}} + \bar{\boldsymbol{a}}' + \bar{\boldsymbol{a}}'' \tag{38}$$

Therefore, a necessary condition for this adiabatic deformation is the existence of $\boldsymbol{a}'$, such that

$$\boldsymbol{b}^{\mathrm{BdG}} - \boldsymbol{b}^{\mathrm{vac}} = \bar{\boldsymbol{a}}' - \boldsymbol{a}' \tag{39}$$

That is, the mismatch in Eq. 36 of the form $\bar{\boldsymbol{a}}' - \boldsymbol{a}'$ can be resolved by including trivial DOFs. This is also what we have done for the doubled Kitaev model in the "Examples" section. Note that $\bar{\boldsymbol{a}}''$ is canceled out from Eq. 39. Therefore, the trivial DOF in Eq. 21 with the same sign of $\mathbb{1}_{D''}$ on both sides of the equation does not help as far as space group representations are concerned.

Completeness of trivial limits

The above vector $\boldsymbol{a}'$ corresponds to the atomic limit of an insulator in class A, AI, or AII depending on the assumption on the time-reversal symmetry in $H_{\boldsymbol{k}}^{\mathrm{BdG}}$. As discussed in detail in (*14*), there are generally a variety of distinct atomic insulators in the presence of spatial symmetries. An atomic insulator can be specified by the position of the localized orbitals and the orbital character. These choices specify a representation $U_{\boldsymbol{k}}(g)'$ of $G_{\boldsymbol{k}}$ for each atomic insulator, and we write its representation count as $\boldsymbol{a}_j$ (j labels distinct atomic insulators). The set

$$\{\mathrm{AI}\} = \left\{ \sum_j \ell_j \boldsymbol{a}_j \,|\, \ell_j \in \mathbb{Z} \right\} \tag{40}$$

is like a finite-dimensional vector space, except that the scalars are integers. We take a basis $\boldsymbol{a}_i$ ($i = 1,2,\ldots,d$) of {AI}.

Viewed as the representation counts in the valence bands of an insulator, it was proven in (*14*) that $\boldsymbol{b}^{\mathrm{BdG}}$ can always be expanded in terms of $\boldsymbol{a}_i$'s using fractional (or integer) coefficients

$$\boldsymbol{b}^{\mathrm{BdG}} = \sum_i q_i \boldsymbol{a}_i,\ q_i \in \mathbb{Q} \tag{41}$$

Since the left-hand side is integer valued, only special values of rational numbers are allowed. The relation Eq. 41 was the fundamental basis of the SIs for topological insulators. Here, we extend the argument for TSCs by proving that $\boldsymbol{b}^{\mathrm{BdG}} - \boldsymbol{b}^{\mathrm{vac}}$ can always be expanded in the following form

$$\boldsymbol{b}^{\mathrm{BdG}} - \boldsymbol{b}^{\mathrm{vac}} = \sum_i c_i (\boldsymbol{a}_i - \bar{\boldsymbol{a}}_i),\ c_i \in \mathbb{Q} \tag{42}$$

Readers not interested in the detail of the proof can skip to the "Quotient group" section.

To demonstrate Eq. 42, note first that $\boldsymbol{b}^{\mathrm{vac}}$ belongs to {AI} and thus can be expanded as

$$\boldsymbol{b}^{\mathrm{vac}} = \sum_i p_i \boldsymbol{a}_i,\ p_i \in \mathbb{Z} \tag{43}$$

Also, Eqs. 41 and 43 imply that $\bar{\boldsymbol{b}}^{\mathrm{BdG}} = \sum_i q_i \bar{\boldsymbol{a}}_i$ and $\bar{\boldsymbol{b}}^{\mathrm{vac}} = \sum_i p_i \bar{\boldsymbol{a}}_i$, which can be verified using Eq. 31. Then it follows that

$$\begin{aligned} \boldsymbol{b}^{\mathrm{BdG}} - \boldsymbol{b}^{\mathrm{vac}} &= \sum_i (q_i - p_i)\boldsymbol{a}_i \\ &= \frac{1}{2}\sum_i \left[(q_i - p_i)(\boldsymbol{a}_i - \bar{\boldsymbol{a}}_i) + (q_i - p_i)(\boldsymbol{a}_i + \bar{\boldsymbol{a}}_i) \right] \end{aligned} \tag{44}$$

The second term vanishes because $\sum_i (q_i - p_i)(\boldsymbol{a}_i + \bar{\boldsymbol{a}}_i) = (\boldsymbol{b}^{\mathrm{BdG}} + \bar{\boldsymbol{b}}^{\mathrm{BdG}}) - (\boldsymbol{b}^{\mathrm{vac}} + \bar{\boldsymbol{b}}^{\mathrm{vac}})$ and because of Eq. 34. Therefore, c_i in Eq. 42 is given by $(q_i - p_i)/2$.

Quotient group

Given a BdG Hamiltonian $H_{\boldsymbol{k}}^{\mathrm{BdG}}$ with a set of assumed symmetries, we can separately compute $\boldsymbol{b}^{\mathrm{BdG}}$ and $\boldsymbol{b}^{\mathrm{vac}}$ and deduce $\boldsymbol{b}^{\mathrm{BdG}} - \boldsymbol{b}^{\mathrm{vac}}$. Distinct BdG Hamiltonians with the same symmetry setting may have different values of $\boldsymbol{b}^{\mathrm{BdG}} - \boldsymbol{b}^{\mathrm{vac}}$. Let us introduce the group $\{\mathrm{BS}\}^{\mathrm{BdG}}$ as the set of all possible $\boldsymbol{b}^{\mathrm{BdG}} - \boldsymbol{b}^{\mathrm{vac}}$ realizable using a BdG Hamiltonian in this symmetry class.

The discussion in the "Symmetry obstructions" section clarified that, as far as the symmetry obstruction in Eq. 39 is concerned, the difference in $\{\mathrm{BS}\}^{\mathrm{BdG}}$ by the combination $\bar{\boldsymbol{a}}' - \boldsymbol{a}'$ is unimportant. Hence, it makes sense to introduce the following subgroup of $\{\mathrm{BS}\}^{\mathrm{BdG}}$

$$\{\mathrm{AI}\}^{\mathrm{BdG}} = \left\{ \sum_i \ell_i (\boldsymbol{a}_i - \bar{\boldsymbol{a}}_i) | \ell_i \in \mathbb{Z} \right\} \tag{45}$$

When $\boldsymbol{b}^{\mathrm{BdG}} - \boldsymbol{b}^{\mathrm{vac}} \in \{\mathrm{BS}\}^{\mathrm{BdG}}$ does not belong to $\{\mathrm{AI}\}^{\mathrm{BdG}}$, the condition Eq. 39 is violated and any smooth deformation in Eq. 21 is prohibited. Such nontrivial values of $\boldsymbol{b}^{\mathrm{BdG}} - \boldsymbol{b}^{\mathrm{vac}}$ can be classified by the quotient group

$$X^{\mathrm{BdG}} \equiv \frac{\{\mathrm{BS}\}^{\mathrm{BdG}}}{\{\mathrm{AI}\}^{\mathrm{BdG}}} \tag{46}$$

This is what we call the refined SI group in this work, which extends the idea in (*20*) to more general symmetry classes.

As we proved in the previous section, $\boldsymbol{b}^{\mathrm{BdG}} - \boldsymbol{b}^{\mathrm{vac}}$ of a given BdG Hamiltonian $H_{\boldsymbol{k}}^{\mathrm{BdG}}$ can be expanded as Eq. 42. Conversely, a vector $\boldsymbol{b}^{\mathrm{BdG}} - \boldsymbol{b}^{\mathrm{vac}}$ given in the form of right-hand side of Eq. 42 has a realization using some BdG Hamiltonian $H_{\boldsymbol{k}}^{\mathrm{BdG}}$ as far as $\boldsymbol{b}^{\mathrm{BdG}} - \boldsymbol{b}^{\mathrm{vac}}$ is integer valued and is consistent with the time-reversal symmetry. This implies that X^{BdG} takes the form $\mathbb{Z}_{n1} \times \mathbb{Z}_{n2} \times \cdots$ (i.e., it contains only torsion factors) and that the actual calculation of X^{BdG} can be done by the Smith decomposition of $\{\mathrm{AI}\}^{\mathrm{BdG}}$ without explicitly constructing $\{\mathrm{BS}\}^{\mathrm{BdG}}$ (*14*).

Relation to previous approach

In previous works (*19*, *36*), $\boldsymbol{b}^{\mathrm{BdG}}$ was viewed as the representation counts in the valence bands of an insulator and was analyzed in the same way as for class A, AI, or AII. In this approach, $\boldsymbol{b}^{\mathrm{BdG}}$ is directly compared against atomic limits $\boldsymbol{a}_i$ (discussed in the "Completeness of trivial limits" section) of the same symmetry setting. When $\boldsymbol{b}^{\mathrm{BdG}}$ cannot be written as a superposition of $\boldsymbol{a}_i$'s with integer coefficients (i.e., $\boldsymbol{b}^{\mathrm{BdG}} \notin \{\mathrm{AI}\}$), then it is said to be nontrivial. This is a sufficient condition for violating all of Eqs. 36, 37, and 39. However, this requirement may be too strong in that, even when $\boldsymbol{b}^{\mathrm{BdG}} \in \{\mathrm{AI}\}$, it would still be possible that $\boldsymbol{b}^{\mathrm{BdG}} - \boldsymbol{b}^{\mathrm{vac}} \notin \{\mathrm{AI}\}^{\mathrm{BdG}}$ and $\boldsymbol{b}^{\mathrm{BdG}} - \boldsymbol{b}^{\mathrm{vac}}$ belongs to the nontrivial class of X^{BdG}. We will see an example of this in the "Example" subsection of the "Refined symmetry-indicators for superconductors" section.

Weak pairing assumption

When applying these methods in the actual search for candidate materials of TSCs, it would be more useful if the input data are only the representation count in the band structure of the normal phase described by $H_{\boldsymbol{k}}$, not in the quasiparticle spectrum of $H_{\boldsymbol{k}}^{\mathrm{BdG}}$. Such a reduction is achieved in (*19*), relying on the weak pairing assumption (*24*, *28*, *29*). This assumption states that $(n_{\boldsymbol{k}}{}^{\alpha})^{\mathrm{BdG}}$ in the superconducting phase does not change even if the limit $\Delta_{\boldsymbol{k}} \to 0$ is taken.

To explain how it works, let $\psi_{\boldsymbol{k}}$ be an eigenstate of $H_{\boldsymbol{k}}$ with the energy $\epsilon_{\boldsymbol{k}}$ belonging to the representation $u_{\boldsymbol{k}}^{\alpha}$ of $G_{\boldsymbol{k}}$. Then, the eigenstate $\psi_{-\boldsymbol{k}}^{*}$ of $-H_{-\boldsymbol{k}}^{*}$ has the energy $-\epsilon_{-\boldsymbol{k}}$ and the representation $u_{\boldsymbol{k}}^{\bar{\alpha}}$ of $G_{\boldsymbol{k}}$, defined in Eq. 29. Thus, representations appearing in the negative-energy quasiparticle spectrum of $H_{\boldsymbol{k}}^{\mathrm{BdG}}$ can be decomposed into the occupied bands (occ) of $H_{\boldsymbol{k}}$ and unoccupied bands (unocc) of $H_{-\boldsymbol{k}}$:

$$\begin{aligned}(n_{\boldsymbol{k}}^{\alpha})^{\mathrm{BdG}} &= n_{\boldsymbol{k}}^{\alpha}|_{\mathrm{occ}} + n_{-\boldsymbol{k}}^{\bar{\alpha}}|_{\mathrm{unocc}} \\ &= (n_{\boldsymbol{k}}^{\alpha} - n_{-\boldsymbol{k}}^{\bar{\alpha}})|_{\mathrm{occ.}} + n_{-\boldsymbol{k}}^{\bar{\alpha}}|_{\mathrm{occ+unocc}}\end{aligned} \tag{47}$$

The last term of this expression is precisely $(n_{\boldsymbol{k}}^{\alpha})^{\mathrm{vac}}$ defined in Eq. 33 This was pointed out recently by (*20*) for the case of inversion symmetry, and we see here that it applies to more general symmetry setting. After all, components of $\boldsymbol{b}^{\mathrm{BdG}} - \boldsymbol{b}^{\mathrm{vac}}$ are given by

$$(n_{\boldsymbol{k}}^{\alpha})^{\mathrm{BdG}} - (n_{\boldsymbol{k}}^{\alpha})^{\mathrm{vac}} = (n_{\boldsymbol{k}}^{\alpha} - n_{-\boldsymbol{k}}^{\bar{\alpha}})|_{\mathrm{occ.}} \tag{48}$$

The last expression is purely the occupied band contribution of the normal-phase band structure, which may be calculated, for example, using the density functional theory (*19*).

We remark that our sense of "weak pairing" is less stringent than that used in (*24*), in that arbitrary inter-Fermi surface pairing is allowed so long as the normal-state energy at the high-symmetry momenta is sufficiently far away from the Fermi surface when compared with the pairing scale.

Example

As an example of SIs for SCs, let us discuss again the Kitaev chain, focusing on its inversion parities. Similar exercise has already been performed in (*20*, *21*), but here we repeat it in our notation to clarify the difference in the present and previous approaches.

For the Kitaev chain with the inversion symmetry, the BdG Hamiltonian is given by $H_{\boldsymbol{k}}^{\mathrm{BdG}}$ with Eq. 22, and the symmetry representation is Eq. 7 with $U_{\boldsymbol{k}}(I) = 1$ and $\chi_I = -1$. For this model, we get

$$\boldsymbol{b}^{\mathrm{BdG}} = (n_0^{+}, n_0^{-}, n_\pi^{+}, n_\pi^{-}) = (1,0,0,1) \tag{49}$$

where $\alpha = \pm$ of n_k^{α} corresponds to the inversion parity. The vacuum limit uses $\chi_I U_k(I)^* = -1$ at both $k = 0$ and π and, thus, has $\boldsymbol{b}^{\mathrm{vac}} = (0,1,0,1)$. Therefore, we find

$$\boldsymbol{b}^{\mathrm{BdG}} - \boldsymbol{b}^{\mathrm{vac}} = (1,0,0,1) - (0,1,0,1) = (1,-1,0,0) \tag{50}$$

For inversion symmetric 1D models in class A, {AI} is a 3D space spanned by

$$\boldsymbol{a}_1 = (1,0,1,0), \boldsymbol{a}_2 = (0,1,0,1), \boldsymbol{a}_3 = (1,0,0,1) \tag{51}$$

For these basis vectors, we find

$$\boldsymbol{a}_1 - \bar{\boldsymbol{a}}_1 = (1,0,1,0) - (0,1,0,1) = (1,-1,1,-1) \tag{52}$$

$$\boldsymbol{a}_2 - \bar{\boldsymbol{a}}_2 = (0,1,0,1) - (1,0,1,0) = (-1,1,-1,1) \tag{53}$$

$$\boldsymbol{a}_3 - \bar{\boldsymbol{a}}_3 = (1,0,0,1) - (0,1,1,0) = (1,-1,-1,1) \tag{54}$$

Since $\boldsymbol{a}_1 - \bar{\boldsymbol{a}}_1 = -(\boldsymbol{a}_2 - \bar{\boldsymbol{a}}_2)$, $\{\mathrm{AI}\}^{\mathrm{BdG}}$ is a 2D space spanned by $\boldsymbol{a}_1 - \bar{\boldsymbol{a}}_1$ and $\boldsymbol{a}_3 - \bar{\boldsymbol{a}}_3$. We find

$$\boldsymbol{b}^{\mathrm{BdG}} - \boldsymbol{b}^{\mathrm{vac}} = \frac{1}{2}(\boldsymbol{a}_1 - \bar{\boldsymbol{a}}_1) + \frac{1}{2}(\boldsymbol{a}_3 - \bar{\boldsymbol{a}}_3) \notin \{\mathrm{AI}\}^{\mathrm{BdG}} \tag{55}$$

The fractional coefficients imply the nontrivial topology of $H_{\boldsymbol{k}}^{\mathrm{BdG}}$. That is, the quotient group in Eq. 46 is $X^{\mathrm{BdG}} = \mathbb{Z}_2$, and $\boldsymbol{b}^{\mathrm{BdG}} - \boldsymbol{b}^{\mathrm{vac}}$ of the present model belongs to the nontrivial class of X^{BdG}.

In contrast, we see that

$$\boldsymbol{b}^{\mathrm{BdG}} = \boldsymbol{a}_3 \in \{\mathrm{AI}\} \tag{56}$$

More generally, the quotient group in one dimension is always trivial for class A, AI, or AII (*14*), meaning that all $\boldsymbol{b}^{\mathrm{BdG}}$ vectors can be expanded by $\boldsymbol{a}_i$'s with integer coefficients. This implies that one cannot detect the nontrivial topology of $H_{\boldsymbol{k}}^{\mathrm{BdG}}$ in 1D based on representations alone in the previous approach.

RESULTS

Interpretation of computed symmetry indicators for superconductors

Using the refined scheme explained in the "Refined symmetry indicators for superconductors" section, we perform a comprehensive computation of X^{BdG} for all space groups G and 1D representations χ_g of superconducting gap functions. The full lists of the results are included in section S1 for both spinful and spinless electrons with or without time-reversal symmetry. The corresponding AZ symmetry classes are listed in Table 1. Most of the nontrivial entries of X^{BdG} can be understood as supergroup of a countable number of key space groups discussed in section S2.

In this section, we discuss the meaning of X^{BdG} using two illuminating examples of $G = P4$ and $P4/m$ in class DIII. Below, we write the component of $\boldsymbol{b}^{\mathrm{BdG}} - \boldsymbol{b}^{\mathrm{vac}}$ as

$$N_{\boldsymbol{k}}^{\alpha} \equiv (n_{\boldsymbol{k}}^{\alpha})^{\mathrm{BdG}} - (n_{\boldsymbol{k}}^{\alpha})^{\mathrm{vac}} \tag{57}$$

In addition, we use the standard labeling of irreducible representations in the literature for χ_g (*37*).

P4 with B representation

The space group $P4$ contains the fourfold rotation symmetry C_4 in addition to the lattice translation symmetries. The B representation refers to the 1D representation of C_4 with $\chi_{C_4} = -1$.

Table 1. Settings used in the calculation for refined SIs and the corresponding AZ symmetry classes.

Spin	Time-reversal symmetry	AZ classes
Spinful	−1	DIII
Spinless	+1	BDI, CI
Spinful	0	D
Spinless	0	D, C

In two spatial dimensions, we find $X^{\mathrm{BdG}} = \mathbb{Z}_2$. To see the meaning of this, let us introduce

$$\nu_{C_4} \equiv \frac{1}{2\sqrt{2}} \sum_{\boldsymbol{k}\in\Gamma,M} \sum_{\alpha=\pm1,\pm3} e^{i\frac{\pi\alpha}{4}} N_{\boldsymbol{k}}^{\alpha} \bmod 2 \tag{58}$$

where $N_{\boldsymbol{k}}^{\alpha}$ represents the number of irreducible representations in Eq. 57 with the fourfold rotation eigenvalue $e^{i\frac{\pi\alpha}{4}}$ at $\Gamma = (0,0)$ and $M = (\pi, \pi)$. As we discuss in the "Indicators for Wannierizable topological superconductors" section, ν_{C_4} turns out to measure the $\mathbb{Z}_2$ QSH index. This was unexpected, because known diagnosis of the QSH index in class AII required either the inversion symmetry I (*30*) or the rotoinversion symmetry S_4 (*11*, *38*), and any proper rotation was not sufficient. Second-order TSCs with a corner Majorna zero mode are also stable under this symmetry setting but are not diagnosed by representations alone, as we discuss in the "Indicators for Wannierizable topological superconductors" section.

In three spatial dimensions, $X^{\mathrm{BdG}} = \mathbb{Z}_2$ detects the weak topological phase of 2D TSCs stacked along the rotation axis z. The strong $\mathbb{Z}_2$ phase of class DIII is prohibited because the $\mathbb{Z}_2$ index of $k_z = 0$ and $k_z = \pi$ planes are forced to be the same by the rotation symmetry C_4.

P4/m

The space group $P4/m$ contains both the inversion I about the origin and the fourfold rotation C_4 around the z axis. The mirror symmetry about the xy plane and fourfold rotoinversion symmetry are given as their products. There are four real 1D representations: A_g ($\chi_{C_4} = +1$, $\chi_I = +1$), A_u ($\chi_{C_4} = +1$, $\chi_I = -1$), B_u ($\chi_{C_4} = -1$, $\chi_I = -1$), and B_g ($\chi_{C_4} = -1$, $\chi_I = +1$). For the A_g representation, X^{BdG} is trivial. We discuss the other three representations one by one. In this section, we denote six high-symmetry points by $\Gamma = (0,0,0)$, $Z = (0,0,\pi)$, $X = (\pi,0,0)$, $R = (\pi,0,\pi)$, and $A = (\pi,\pi,\pi)$ (*39*).

A_u representation ($\chi_{C_4} = +1$, $\chi_I = -1$). Let us start with the A_u representation. Although X^{BdG} in 3D is large (see Table 2), many factors can be attributed to lower dimensions.

In a 1D system along the rotation axis, we find $X^{\mathrm{BdG}} = (\mathbb{Z}_2)^2$, which can be characterized by

$$\nu_{1/2}^{\mathrm{1D}} = \frac{1}{4} \sum_{\boldsymbol{k}=\Gamma,Z} \sum_{\alpha=\pm1} (N_{\boldsymbol{k}}^{\alpha,+} - N_{\boldsymbol{k}}^{\alpha,-}) \bmod 2 \tag{59}$$

$$\nu_{3/2}^{\mathrm{1D}} = \frac{1}{4} \sum_{\boldsymbol{k}=\Gamma,Z} \sum_{\alpha=\pm3} (N_{\boldsymbol{k}}^{\alpha,+} - N_{\boldsymbol{k}}^{\alpha,-}) \bmod 2 \tag{60}$$

where $N_{\boldsymbol{k}}^{\alpha,\beta}$ represents the number of irreducible representations with the C_4 eigenvalue $e^{i\frac{\alpha\pi}{4}}$ and the inversion parity $\beta = \pm1$ at Γ and Z. They measure the number of Majorana edge modes with different rotation eigenvalues.

Table 2. List of X^{BdG} for class DIII systems with $P\bar{1}$ (*20*), *P4*, and *P4/m* symmetry in each spatial dimension.

SG (rep of Δ_k)	1D	2D	3D
$P\bar{1}$ (A_u)	$\mathbb{Z}_2$	$(\mathbb{Z}_2)^2 \times \mathbb{Z}_4$	$(\mathbb{Z}_2)^3 \times (\mathbb{Z}_4)^3 \times \mathbb{Z}_8$
P4 (B)	$\mathbb{Z}_1$	$\mathbb{Z}_2$	$\mathbb{Z}_2$
P4/m (A_u)	$(\mathbb{Z}_2)^2$	$\mathbb{Z}_2 \times \mathbb{Z}_8$	$(\mathbb{Z}_2)^4 \times \mathbb{Z}_4 \times \mathbb{Z}_8 \times \mathbb{Z}_{16}$
P4/m (B_u)	$\mathbb{Z}_1$	$\mathbb{Z}_2 \times \mathbb{Z}_8$	$\mathbb{Z}_2 \times (\mathbb{Z}_4)^2 \times \mathbb{Z}_8$
P4/m (B_g)	$\mathbb{Z}_1$	$(\mathbb{Z}_2)^2$	$(\mathbb{Z}_2)^3$

In mirror-invariant 2D planes orthogonal to the z axis, we find $X^{\mathrm{BdG}} = \mathbb{Z}_2 \times \mathbb{Z}_8$. The $\mathbb{Z}_2$ factor is given by

$$\nu_x^{\mathrm{1D}} = \frac{1}{4} \sum_{\beta=\pm1} \left(\sum_{\alpha=\pm1,\pm3} \beta N_{\Gamma}^{\alpha,\beta} + \sum_{\alpha=\pm2} \beta N_X^{\alpha,\beta} \right) \tag{61}$$

where $N_X^{\pm2,\beta}$ represents the number of irreducible representations with the C_2 eigenvalue $\pm i$ and the inversion parity $\beta = \pm1$ at X. The phase with ν_x^{1D} corresponds to 1D Kitaev chains stacked along x and y axes. The $\mathbb{Z}_8$ factor is related to TSCs with mirror Chern number C_{M} and second-order TSCs. It is given by (*38*).

$$\begin{aligned} z_8 \;=\; & -\frac{3}{2}N_{\Gamma}^{-3,+} + \frac{3}{2}N_{\Gamma}^{3,-} + \frac{1}{2}N_{\Gamma}^{1,+} - \frac{1}{2}N_{\Gamma}^{-1,-} \\ & -\frac{3}{2}N_{M}^{-3,+} + \frac{3}{2}N_{M}^{3,-} + \frac{1}{2}N_{M}^{1,+} \\ & -\frac{1}{2}N_{M}^{-1,-} - N_{X}^{2,+} + N_{X}^{-2,-} \bmod 8 \end{aligned} \tag{62}$$

This formula rewrites the one for the mirror Chern number in the form of summation. Thus, z_8 equals to C_M mod 4 (*40*). To see the meaning of $z_8 = 4$ mod 8, we generate an example of phases with $(\nu_x^{\mathrm{1D}}, z_8) = (1,4)$ by the wire construction as illustrated in Fig. 2A. Keeping both the inversion and the rotation symmetry but breaking the translation symmetry, one can gap out edges, realizing a second-order TSC that features two zero modes with different chirality at each of four corners. We can also generate a phase with $(\nu_x^{\mathrm{1D}}, z_8) = (0,4)$ by stacking four copies of mirror Chern insulator with $C_M = 1$. From these observations, we conclude

$$C_{\mathrm{M}} \;=\; 4\nu_2 + z_8 + 8\mathbb{Z} \tag{63}$$

where $\nu_2 = 0$ and 1 is the index for the second-order TSC.

Last, we discuss 3D systems. The $(\mathbb{Z}_2)^4 \times \mathbb{Z}_4 \times \mathbb{Z}_8$ part of X^{BdG} originates from lower dimensions. For example, ν_x^{1D} in Eq. 61 for the $k_z = 0$ plane gives a $\mathbb{Z}_2$ factor, and $\nu_{1/2}^{\mathrm{1D}}$ in Eq. 59 and $\nu_{3/2}^{\mathrm{1D}}$ in Eq. 60 for the two fourfold symmetric lines (the $\Gamma - Z$ line and the M-A line) produce four $\mathbb{Z}_2$ factors, but only three of them are independent from other indices. The $\mathbb{Z}_4$ factor can be accounted for by the inversion parity

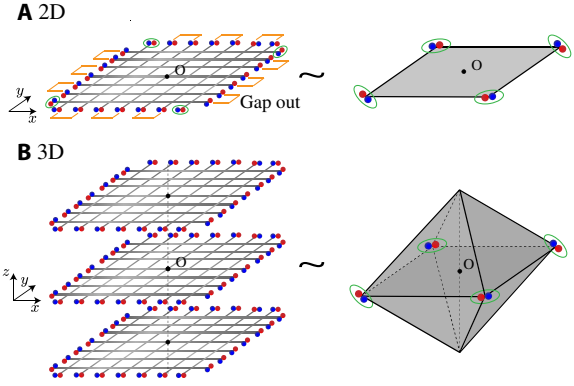

Fig. 2. Examples of wire construction for *P4/m* realizing higher-order TSCs with Majorana corner modes (circled by green ellipses). (**A**) $(\nu_x^{\mathrm{1D}}, z_8) = (1,4)$ phase in 2D. Orange marks represent translation-breaking perturbations on the edge, gapping out pairs of zero modes. (**B**) $(z_{8,k_z=0}, z_{8,k_z=\pi}, z_{16}) = (4,4,8)$ phase in 3D.

$$\frac{1}{4}\sum_{\beta=\pm1}\Big(\sum_{\boldsymbol{k}=\Gamma,Z}\sum_{\alpha=\pm1,\pm3}\beta N_{\boldsymbol{k}}^{\alpha,\beta}+\sum_{\boldsymbol{k}\in X,R}\sum_{\alpha=\pm2}\beta N_{\boldsymbol{k}}^{\alpha,\beta}\Big) \tag{64}$$

The $\mathbb{Z}_8$ factor is given by the index z_8 in Eq. 62 for the $k_z = \pi$ plane.

To explain the remaining $\mathbb{Z}_{16}$ factor, we introduce a strong $\mathbb{Z}_{16}$ index defined by

$$z_{16} = \kappa_1 - 2\kappa_4 \bmod 16, \tag{65}$$

$$\kappa_1 = \frac{1}{4}\sum_{\beta=\pm1}\Big(\sum_{\boldsymbol{k}=\Gamma,Z,M,A}\sum_{\alpha=\pm1,\pm3}\beta N_{\boldsymbol{k}}^{\alpha,\beta}+2\sum_{\boldsymbol{k}\in X,R}\sum_{\alpha=\pm2}\beta N_{\boldsymbol{k}}^{\alpha,\beta}\Big) \tag{66}$$

$$\kappa_4 = \frac{1}{2\sqrt{2}}\sum_{\boldsymbol{k}\in K_4}\sum_{\alpha=\pm1,\pm3}(e^{i\frac{\pi\alpha}{4}}N_{\boldsymbol{k}}^{\alpha,+}-e^{i\frac{\pi\alpha}{4}}N_{\boldsymbol{k}}^{\alpha,-}) \tag{67}$$

where K_4 represents the set of four high-symmetry momenta invariant under S_4. We find that $z_{16} = 0$ mod 16 holds for all elements in $\{\mathrm{AI}\}^{\mathrm{BdG}}$. This z_{16} invariant, when focused on its "mod 8" part, has the same implication as for class AII systems (*11*, *38*). Namely, z_{16} mod 4 agrees with the mirror Chern number, and $z_{16} = 4$ mod 8 implies a second-order TSC. To investigate the topology of phases with $z_{16} = 8$ mod 16, we stack 2D second-order TSCs with $z_8 = 4$ and $C_M = 0$ as illustrated in Fig. 2B. The value of z_{16} depends on how to stack the 2D layers since z_{16} is related to the z_8 index for the $k_z = 0$ and π planes as

$$z_{16} = -(z_{8,k_z=0} + z_{8,k_z=\pi}) \tag{68}$$

If the inversion center is contained in a layer (i.e., there exists a single layer left invariant under the inversion), $z_{16} = 8$ and the system exhibits Majorana corner states. If, on the other hand, the inversion center is not contained in any layer, $z_{16} = 0$ and the surface can be completely gapped without breaking symmetries or closing the bulk gap. Phases with $z_{16} = 8$ mod 16 can also be mirror Chern TSCs just like in the 2D case.

B_u representation ($\chi_{C_4} = -1, \chi_I = -1$). Next, let us consider the B_u representation. In one dimensions, we found X^{BdG} is trivial. This is because the fourfold rotation symmetry together with the choice $\chi_{C_4} = -1$ implies that the $\mathbb{Z}_2$ index of class DIII is trivial.

In two dimensions, the interpretation of $X^{\mathrm{BdG}} = \mathbb{Z}_2 \times \mathbb{Z}_8$ is the same as the A_u representation, but the formula for z_8 index must be replaced by

$$z_8' = \sum_{\boldsymbol{k}\in\Gamma,M}(N_{\boldsymbol{k}}^{3,+}+3N_{\boldsymbol{k}}^{3,-})+2N_X^{2,-} \bmod 8 \tag{69}$$

In three dimensions, the $\mathbb{Z}_2 \times \mathbb{Z}_4 \times \mathbb{Z}_8$ part of X^{BdG} is weak indices. The remaining $\mathbb{Z}_4$ factor can be explained by κ_1 in Eq. 66.

The QSH indices of the $k_z = 0$ and $k_z = \pi$ planes must be the same since rotation eigenvalues on these planes must coincide due to the compatibility relations along rotation-symmetric lines. Therefore κ_1 (defined modulo 8) is restricted to be even and characterizes the $\mathbb{Z}_4$ factor. For the B_u representation, κ_4 always vanishes and $z_{16} = \kappa_1$. Since Eq. 68 still holds, $\kappa_1 = 2$ mod 4 implies a nontrivial mirror Chern number. As discussed in section S3, there are no third-order TSCs in this symmetry setting. With these results, we conclude that $\kappa_1 = 4$ mod 8 also indicates a nonzero mirror Chern number.

B_g representation ($\chi_{C_4} = -1, \chi_I = +1$). Last, let us discuss B_g representation. In this case, the mirror symmetry commutes with the particle-hole symmetry ($\chi_M = \chi_{C_4}^2\chi_I = +1$), and the mirror Chern number must vanish (*41*).

In two dimensions, we find $X^{\mathrm{BdG}} = \mathbb{Z}_2 \times \mathbb{Z}_2$. These class are characterized by

$$\nu_{C_4}^{+} = \frac{1}{2\sqrt{2}}\sum_{\boldsymbol{k}\in\Gamma,M}\sum_{\alpha=\pm1,\pm3}e^{i\frac{\pi\alpha}{4}}N_{\boldsymbol{k}}^{\alpha,+} \bmod 2 \tag{70}$$

$$\nu_{C_4}^{-} = \frac{1}{2\sqrt{2}}\sum_{\boldsymbol{k}\in\Gamma,M}\sum_{\alpha=\pm1,\pm3}e^{i\frac{\pi\alpha}{4}}N_{\boldsymbol{k}}^{\alpha,-} \bmod 2 \tag{71}$$

where $N_{\boldsymbol{k}}^{\alpha,\beta}$ represents the number of irreducible representations with the C_4 eigenvalue $e^{i\frac{\pi\alpha}{4}}$ and the inversion parity $\beta = \pm1$ at $\Gamma = (0,0)$ and $M = (\pi, \pi)$. Phases with $(\nu_{C_4}^{+}, \nu_{C_4}^{-}) = (1,0)$ or $(0,1)$ turn out to be gapless. An example of the quasiparticle spectrum is shown in Fig. 3A. To see why, recall that $\nu_{C_4} = \nu_{C_4}^{+} + \nu_{C_4}^{-} = 1$ mod 2 implies the nontrivial $\mathbb{Z}_2$ QSH index as discussed in the "*P*4 with *B* representation" section. However, when $\chi_I = +1$, the QSH index cannot be nontrivial (*28*). The only way out is the gap closing of the quasiparticle spectrum, which invalidates the definition of the QSH index. Phases with $(1,1) \in \mathbb{Z}_2 \times \mathbb{Z}_2$ can be gapped, and they are second-order TSCs.

Last, we discuss 3D systems. For B_g representation, κ_1 should always be 0, while κ_4 can be nonzero. It is restricted to be even, explaining the strong $\mathbb{Z}_2$ factor in X^{BdG}. As explained in the Supplementary Materials, $\kappa_4 = 2$ mod 4 indicates second-order TSCs.

Example

To demonstrate the prediction of SIs, let us discuss a simple 2D model with *P*4/*m* symmetry. The BdG Hamiltonian $H_{\boldsymbol{k}}^{\mathrm{BdG}}$ is given by Eq. 1 with

$$H_{\boldsymbol{k}} = -(\cos k_x + \cos k_y + 1)\mathbb{1}_2 \tag{72}$$

$$\Delta_{\boldsymbol{k}} = (\cos k_x - \cos k_y)\, i\sigma_2 \tag{73}$$

Here, σ_i's are the Pauli matrices. The inversion symmetry and the fourfold rotation symmetry are represented by

$$U_{\boldsymbol{k}}(I) = \mathbb{1}_2, \chi_I = +1 \tag{74}$$

$$U_{\boldsymbol{k}}(C_4) = e^{-i\frac{\pi}{4}\sigma_3}, \chi_{C_4} = -1 \tag{75}$$

Thus, the model belongs to the B_g representation of *P*4/*m* discussed in the "B_g representation ($\chi_{C4} = -1, \chi_I = +1$)" section. We compute the indices in Eqs. 70 and 71 and get $(\nu_{C_4}^{+}, \nu_{C_4}^{-}) = (0,1)$, which suggests nodal points in the quasiparticle spectrum (see Fig. 3A) as discussed in the "B_g representation ($\chi_{C_4} = -1, \chi_I = +1$)" section.

If inversion-breaking perturbations are added, the space group symmetry is reduced to *P*4. Here, we consider the following term

$$\begin{aligned} V_{\boldsymbol{k}}^{\mathrm{BdG}} = {} & \epsilon_1(\sin k_x\sigma_1\tau_0 + \sin k_y\sigma_2\tau_3) \\ & +\epsilon_2(\sin k_x\sigma_0\tau_2 + \sin k_y\sigma_3\tau_1) \end{aligned} \tag{76}$$

The fourfold rotation symmetry remains intact and $\chi_{C4} = -1$. Thus, $\nu_{C_4} = \nu_{C_4}^{+} + \nu_{C_4}^{-} = 1$ is still well defined. For small perturbations, the bulk spectrum remains gapless and flat surface bands [Andreev bound states (*42*)] appear in the surface spectrum (Fig. 3B). As the perturbation strength is increased, the system gets gapped without closing gap at high-symmetry points and becomes a helical TSC (Fig. 3C).

Application to $Cu_xBi_2Se_3$

One of the most studied bulk TSCs is $Cu_xBi_2Se_3$, whose space group is $R\bar{3}m$. The corresponding point group D_{3d} contains the inversion I, the threefold rotation about z axis C_3, and the mirror symmetry about the yz plane M_x. There are several proposals for possible odd-parity pairings. One-dimensional representations A_{1u} ($\chi_I = -1$, $\chi_{M_x} = -1$, $\chi_{C_3} = +1$) and A_{2u} ($\chi_I = -1$, $\chi_{M_x} = +1$, $\chi_{C_3} = +1$) of $R\bar{3}m$ produce the superconducting gap Δ_2 and Δ_3, respectively. When the 2D irreducible representation E_u is used, the point group D_{3d} is reduced to C_{2h} (*43*). Several recent studies have reported a nematic order that spontaneously breaks the threefold rotation C_3, supporting the E_u pairing (*44*). Then, the 2D representation of D_{3d} splits into two 1D representations: A_u ($\chi_I = -1$, $\chi_{M_x} = -1$) and B_u ($\chi_I = -1$, $\chi_{M_x} = +1$) of C_{2h}, corresponding to the superconducting gap Δ_{4y} and Δ_{4x}, respectively (*28*, *44*).

Let us discuss the implication of SIs for each of these odd-parity pairings. First of all, κ_1 (the sum of the inversion parities divided by four; see section S2A) is odd for all of these cases. This can be seen by focusing on the small Fermi surface around Γ that originates from the Cu doping to the topological insulator Bi_2Se_3. On the one hand, this value of κ_1 indicates that the 3D winding number ν_w is odd for gapped SCs. On the other hand, as proven in section S5, there is a relation $\nu_w = -\chi_{M_x}\nu_w$ among ν_w and χ_{M_x}. Therefore, we conclude that Δ_2 and Δ_{4y} can be a gapped TSC with a nontrivial winding, and Δ_3 and Δ_{4x} must contain SC nodes. According to (*45*), the Δ_{4x} pairing contains Dirac nodes protected by the mirror symmetry.

Indicators for WTSCs

So far, we have mostly focused on the formalism and physical meaning of the refined SIs for superconductors. From the discussions on the Kitaev chain in (*20*, *21*) and the "Refined symmetry indicators for superconductors" section, one might expect the main power of the SI refinement is to capture TSCs with zero-dimensional surface states. This is untrue: In the "$P4$ with B representation" section, we have already asserted that the C_4-refined SI, ν_{C_4}, actually detects either a gapless phase or the helical TSC in class DIII in two dimensions.

We will substantiate our claim in this section. A general approach for physically interpreting the SIs is to first construct a general set of topological phases protected by the symmetries and then evaluate their SIs to establish the relations between the two (*11*, *38*). We will follow a similar scheme: First, we introduce the notion of WTSC, which, like the Kitaev chain, reduces to an atomic state once the particle-hole symmetries are broken; next, we discuss how particle-hole symmetry restricts the possible associated atomic states that could correspond to a WTSC; and last, we specialize our discussion to 2D superconductors with $\chi_{C_4} = -1$ and show that the nontrivial refined SI does not indicate a WTSC. Our claim follows when the arguments above are combined with the established classification of class AII topological (crystalline) insulators (*6*, *7*, *9*–*13*).

Before moving on, we remark that, insofar as our claim on the physical meaning of ν_{C_4} is concerned, there is probably a simpler approach in which one relates the nontrivial SI $\nu_{C_4} = 1$ to the Fermi-surface invariant in (*24*) under the weak-pairing assumption. Our approach, however, is more general in that the weak-pairing assumption is not required and that the analysis of the SIs corresponding to WTSCs also helps one understand the physical meaning of the SIs, as can be seen in the $P4/m$ examples.

Wannierizable TSCs

Let us begin by introducing the notion of WTSCs. Consider a gapped Hamiltonian. To investigate the possible topological nature of the system, we ask if it is possible to remove all quantum entanglement in the many-body ground state while respecting all symmetries. In the context of noninteracting insulators, this question can be rephrased in the notion of Wannier functions, and we say a phase is topological if there is an obstruction for constructing symmetric, exponentially localized Wannier functions out of the Bloch states below the energy gap (*14*, *15*, *33*).

For superconductors, the question of ground-state quantum entanglement is more subtle even within a mean-field BdG treatment. As a partial diagnosis, we could still apply the same Wannier criterion to the Bloch states below the gap at $E = 0$, and we say a BdG Hamiltonian is "Wannierizable" when no Wannier obstruction exists. [There is a technical question of whether the addition of trivial states below the gap is allowed, which differentiates "stable" topological phases from "fragile" ones (*33*). Since our starting point is a BdG Hamiltonian, the corresponding physical system does not have charge conservation symmetry, and it is more natural to focus on stable topological phases. We will take this perspective and always assume appropriate trivial DOF could be supplied to resolve any possible fragile obstructions in a model.] A non-Wannierizable BdG Hamiltonian is necessarily topological, and phases like the 2D helical TSC in class DIII can be diagnosed that way. However, as the mentioned Wannier criterion uses only Bloch states with energy $E_{\boldsymbol{k}} < 0$, it inherently ignores the presence of particle-hole symmetry when we consider obstructions to forming localized, symmetric Wannier functions, i.e., in the Wannierization, we only demand the subgroup of symmetries that commute with the single-particle Hamiltonian. Because of this limitation, the Wannier criterion does not detect TSCs whose BdG Hamiltonians become trivial when the particle-hole symmetry is ignored, like the Kitaev chain. When a Wannierizable BdG Hamiltonian is topological (in the sense defined in the "Topology of superconductors" section), we call it a WTSC.

Constraints on the associated atomic insulators

By definition, given any Wannierizable BdG Hamiltonian in class DIII, we can define an associated atomic insulator in class AII. On the basis of the recently developed paradigms for the classifications of topological crystalline insulators (*7*, *9*, *10*, *46*), we can consider the associated atomic insulator ψ as an element of a finitely generated Abelian group $\mathcal{C}_{\mathrm{AI}}$. More concretely, let H^{BdG} be Wannierizable, and let $\psi^{\mathrm{BdG}} \in \mathcal{C}_{\mathrm{AI}}$ be the associated atomic insulator. Similar to the formalism for the refined SI, we also consider the limit when the chemical potential approaches $-\infty$. The vacuum is Wannierizable, and so we can also define $\psi^{\mathrm{vac}} \in \mathcal{C}_{\mathrm{AI}}$. In the following, we will again be focusing on the difference $\delta\psi \equiv \psi^{\mathrm{BdG}} - \psi^{\mathrm{vac}} \in \mathcal{C}_{\mathrm{AI}}$.

Although we have ignored the particle-hole symmetry Ξ in discussing the Wannierizability of a BdG Hamiltonian, it casts important constraints on the possible states $\delta\psi \in \mathcal{C}_{\mathrm{AI}}$. Physically, ψ^{vac} can be identified with the states forming the hole bands ($E < 0$) of an empty lattice, and it is determined by the sites, orbitals, as well as the choice on the superconducting pairing symmetry denoted by χ. We can also consider the states forming the electron bands ($E > 0$) of the empty lattice, which are related to ψ by the particle-hole symmetry. More generally, we can define a linear map $\Xi_\chi : \mathcal{C}_{\mathrm{AI}} \to \mathcal{C}_{\mathrm{AI}}$ which relates an atomic insulator with its particle-hole conjugate. Noticing that $\psi^{\mathrm{vac}} + \Xi_\chi[\psi^{\mathrm{vac}}]$ describes the full Hilbert space in our BdG description, we must have

$$\psi^{\mathrm{BdG}} + \Xi_\chi[\psi^{\mathrm{BdG}}] = \psi^{\mathrm{vac}} + \Xi_\chi[\psi^{\mathrm{vac}}] \tag{77}$$

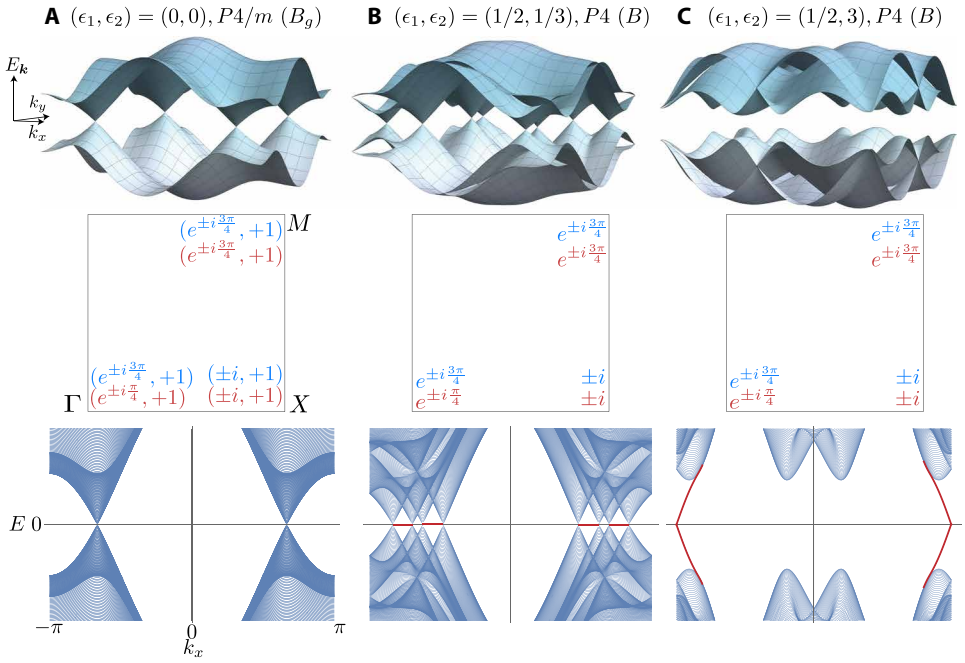

Fig. 3. Quasiparticle spectrum (top), symmetry representations of $E < 0$ states (middle), and the surface band structure (bottom) of $H_{\boldsymbol{k}}^{\mathrm{BdG}}$ with Eqs. 72 and 73. In (**A**), each bands are doubly degenerate due to the inversion and the time-reversal symmetry. For (**B**) and (**C**), inversion-breaking perturbations in Eq. 76 are included. Symmetry representations colored in red is for $H_{\boldsymbol{k}}^{\mathrm{BdG}}$, and those in blue is for H^{vac}. In the surface band structure, states localized near edges are colored in red.

We remark that Eq. 77 parallels Eq. 34 in defining the refined SI. Equation 77 can be rearranged into a condition that $\delta\psi$ has to satisfy

$$(\mathbb{1} + \Xi_\chi)\,\delta\psi \;\equiv\; \delta\psi + \Xi_\chi[\,\delta\psi] = 0 \tag{78}$$

where we denote the identity map by $\mathbb{1}$ and the trivial element of $\mathcal{C}_{\mathrm{AI}}$ by 0. Note that $\Xi_\chi^2 = \mathbb{1}$.

An obvious class of solutions to Eq. 78 is to take $\delta\psi = \psi - \Xi_\chi[\psi]$ for any $\psi \in \mathcal{C}_{\mathrm{AI}}$. Such solutions arise when we take $\psi^{\mathrm{BdG}} = \Xi_\chi[\psi^{\mathrm{vac}}]$, the fully filled state of the system, in the definition of $\delta\psi$. Mathematically, we can view them as elements in the image of the map $\mathbb{1} - \Xi_\chi$, and it is natural for us to quotient out these trivial solutions

$$\mathcal{X}^{\mathrm{WTSC}} \equiv \frac{\mathrm{Ker}\,(\mathbb{1} + \Xi_\chi)}{Im(\mathbb{1} - \Xi_\chi)} \tag{79}$$

If $\delta\psi$ belongs to a nontrivial class in $\mathcal{X}^{\mathrm{WTSC}}$, the gap must close when we change the chemical potential to either one of the limits $\mu \to \pm\infty$, and so the BdG Hamiltonian cannot be trivial. Physically, we interpret $\mathcal{X}^{\mathrm{WTSC}}$ as an indicator for WTSC. Note that, generally, $\mathcal{X}^{\mathrm{WTSC}}$ is only an indicator, not a classification, of WTSCs. This is because $\psi_1 = \psi_2$ is only a necessary, but not generally sufficient, c∈ondition for the existence of a symmetric, adiabatic deformation between two Wannierizable BdG Hamiltonians.

We can now relate $\mathcal{X}^{\mathrm{WTSC}}$ to the refined SI by evaluating the momentum-space symmetry representations of $\delta\psi$. If $\delta\psi$ belongs to the trivial class of $\mathcal{X}^{\mathrm{WTSC}}$, we can write $\delta\psi = \psi - \Xi_\chi[\psi]$ for some $\psi \in \mathcal{C}_{\mathrm{AI}}$. Correspondingly, its representation vector takes the form $\boldsymbol{a} - \bar{\boldsymbol{a}}$ for some $\boldsymbol{a} \in \{\mathrm{AI}\}$, and so its SI will also be trivial. This implies if two atomic mismatches $\delta\psi_1$ and $\delta\psi_2$ belong to the same class in the quotient group $\mathcal{X}^{\mathrm{WTSC}}$, they will have the same refined SI. That is, the evaluation of the refined SI gives a well-defined map $\mathrm{SI} : \mathcal{X}^{\mathrm{WTSC}} \to X^{\mathrm{BdG}}$. Note that the symmetry representations may not detect all topological distinctions between atomic states, and so $\mathrm{SI}[\mathcal{X}^{\mathrm{WTSC}}]$ generally contains less information than $\mathcal{X}^{\mathrm{WTSC}}$.

Observe that $\mathrm{SI}[\mathcal{X}^{\mathrm{WTSC}}]$ is a subgroup of X^{BdG}. If H^{BdG} is Wannierizable, its representation vector $\boldsymbol{b}^{\mathrm{BdG}} - \boldsymbol{b}^{\mathrm{vac}}$ must have an SI in the subgroup $\mathrm{SI}[\mathcal{X}^{\mathrm{WTSC}}]$. Conversely, any SI that does not belong to this subgroup is inconsistent with any WTSC.

Interpretation of νC_4

We can now apply the formalism to show that a 2D BdG Hamiltonian in class DIII with $\nu_{C4} = 1$ cannot be Wannierizable, and hence, it must be either gapless or has a nontrivial $\mathbb{Z}_2$ QSH index (*11*–*13*). Following the general plan described above, we will first compute the group $\mathcal{C}_{\mathrm{AI}}$ classifying the associated atomic insulators, construct the map Ξ_χ corresponding to $\chi_{C_4} = -1$, and, lastly, show that a phase with $\nu_{C4} = 1$ cannot be Wannierizable as $\mathrm{SI}[\mathcal{X}^{\mathrm{WTSC}}] = \mathbb{Z}_1$, the trivial group.

To classify the associated atomic insulators, we first consider the set of possible lattices and orbitals. In 2D with C_4 rotation symmetry, there are four Wyckoff positions: $\mathcal{W}_a = \{(0,0)\}$, $\mathcal{W}_b = \{(1/2,1/2)\}$, $\mathcal{W}_c = \{(1/2,0), (0,1/2)\}$, and $\mathcal{W}_d = \{(x, y), (-y, x), (-x, -y), (y, -x)\}$ being the general position. A site in $\mathcal{W}_a$ or $\mathcal{W}_b$ is symmetric under C_4 rotation, and for spinful fermions with time-reversal symmetry, we can label the orbitals by $\alpha = \pm 1$ or ± 3 characterizing the C_4 eigenvalue $e^{i\frac{\pi\alpha}{4}}$, where the $\pm$ states form a Kramers pair. When the site filling is two, we fill one of the two types of orbitals, and we denote the corresponding atomic insulators by $\psi_{a,b}^{\pm 1}$ and $\psi_{a,b}^{\pm 3}$. Generally, the site-filling may be larger than two, and we denote a state with $2n$ fermions filling orbitals with $\alpha = \pm 1$ and $2m$ with $\alpha = \pm 3$, both in $\mathcal{W}_a$, by the expression $n\psi_a^{\pm 1} + m\psi_a^{\pm 3}$. We can perform the same analysis for $\mathcal{W}_c$ and $\mathcal{W}_d$. A site in $\mathcal{W}_c$ only has C_2 rotation symmetry, and the two possible rotation eigenvalues form a Kramers pair. Since there is only one orbital type, we will denote the corresponding

atomic insulator by ψ_c. Similarly, we will let ψ_d denote the atomic insulator living on the general position.

While we have listed a total of six possible atomic insulators with the minimal filling of two fermions per site, these states are not completely independent. To see why, consider setting the free parameters in the general position $\mathcal{W}_d$ to $x = y = 0$, which corresponds to moving all four sites in the unit cell to the point-group origin. As the deformation of sites can be done in a smooth manner, the atomic insulator ψ_d must be equivalent to an appropriate stack of atomic insulators defined on $\mathcal{W}_a$. Such equivalence can be deduced by studying the point-group symmetry representation furnished by the collapsing sites (*15*, *46*). We can perform a similar analysis by collapsing the sites in $\mathcal{W}_d$ to the other two Wyckoff positions, and altogether, we find the equivalence relations

$$\psi_d \sim 2\psi_a^{\pm 1} + 2\psi_a^{\pm 3} \sim 2\psi_b^{\pm 1} + 2\psi_b^{\pm 3} \sim 2\psi_c \tag{80}$$

As such, any atomic insulator ψ in our setting can be formally expanded as

$$\begin{aligned}\psi &= n_a\psi_a^{\pm 1} + n_b\psi_b^{\pm 1} + n_c\psi_c \\ &+\xi_a(\psi_a^{\pm 1} + \psi_a^{\pm 3} - \psi_c) + \xi_b(\psi_b^{\pm 1} + \psi_b^{\pm 3} - \psi_c)\end{aligned} \tag{81}$$

where $n_{a,b,c} \in \mathbb{Z}$ and $\xi_{a,b} \in \mathbb{Z}_2$. That is, the atomic insulators are classified by the group $\mathcal{C}_{\mathrm{AI}} = \mathbb{Z}^3 \times (\mathbb{Z}_2)^2$. In this language, we represent any (class of) atomic insulator by the collection of integers (n_a, n_b, n_c, ξ_a, ξ_b). For instance,

$$\psi_a^{\pm 1} \mapsto (1,0,0,0,0);\ \psi_a^{\pm 3} \mapsto (-1,0,1,1,0) \tag{82}$$

We are now ready to construct the map Ξ_χ. With the choice of $\chi_{C_4} = -1$, the C_4 rotation eigenvalues of local orbitals related by Ξ differ by −1. As such, the particle-hole acts on the atomic insulators as follows

$$\Xi_\chi[\psi_{a,b}^{\pm 1}] = \psi_{a,b}^{\mp 3};\ \Xi_\chi[\psi_c] = \psi_c \tag{83}$$

and recall that $\Xi_\chi^2 = \mathbb{1}$, the identity. We can equally represent the action of Ξ_χ by a matrix

$$\Xi_\chi\begin{bmatrix}\begin{pmatrix}n_a\\n_b\\n_c\\\xi_a\\\xi_b\end{pmatrix}\end{bmatrix} = \begin{pmatrix}-1&0&0&0&0\\0&-1&0&0&0\\1&1&1&0&0\\1&0&0&1&0\\0&1&0&0&1\end{pmatrix}\begin{pmatrix}n_a\\n_b\\n_c\\\xi_a\\\xi_b\end{pmatrix} \tag{84}$$

We can now compute $\mathcal{X}^{\mathrm{WTSC}}$. On the one hand, we can parameterize elements in Ker $(\mathbb{1} + \Xi_\chi)$ by

$$\delta\psi = (2m_a, 2m_b, -m_a + m_b, \xi_a, \xi_b) \tag{85}$$

where each of $m_{a,b}$, $\xi_{a,b}$ corresponds to a generator, i.e.,

$$\mathrm{Ker}\,(\mathbb{1}+\Xi_\chi) = \mathrm{span}\{(2,0,-1,0,0),(0,2,-1,0,0),(0,0,0,1,0),(0,0,0,0,1)\} \tag{86}$$

This shows that Ker $(\mathbb{1} + \Xi_\chi) \simeq \mathbb{Z}^2 \times (\mathbb{Z}_2)^2$. On the other hand, an element $\delta\psi' \in Im(\mathbb{1} - \Xi_\chi)$ takes the form

$$\delta\psi' = (2n_a, 2n_b, -n_a - n_b, n_a \bmod 2, n_b \bmod 2) \tag{87}$$

and so we can write

$$Im\,(\mathbb{1} - \Xi_\chi) = \mathrm{span}\{(2,0,-1,1,0),(0,2,-1,0,1)\} \tag{88}$$

which is abstractly the group $\mathbb{Z}^2$. Comparing Eq. 87 against Eq. 86, we find the quotient group

$$\mathcal{X}^{\mathrm{WTSC}} = (\mathbb{Z}_2)^2 \tag{89}$$

and we may take (0,0,0,1,0) and (0,0,0,0,1) as representatives of the generating elements.

Last, we evaluate SI$[\mathcal{X}^{\mathrm{WTSC}}]$. The corresponding representation vectors of the atomic states satisfy the relations

$$\boldsymbol{a}_c = \boldsymbol{a}_a^{\pm 1} + \boldsymbol{a}_a^{\pm 3} = \boldsymbol{a}_b^{\pm 1} + \boldsymbol{a}_b^{\pm 3} \tag{90}$$

From this, we conclude SI$[\mathcal{X}^{\mathrm{WTSC}}] = \mathbb{Z}_1$, and so $\nu_{C_4} = 1$ implies the BdG Hamiltonian cannot be Wannierizable.

While the discussion above focuses on a 2D system with C_4 rotation symmetry, one can perform the same analysis for any other symmetry setting. In particular, we tabulate the results for space group $P\bar{1}$ and $P4/m$ under different SC representations in Table 3. For $P\bar{1}$ and $P4/m$, we found SI$[\mathcal{X}^{\mathrm{WTSC}}] = \mathcal{X}^{\mathrm{WTSC}}$, and nontrivial entries correspond to WTSCs like stacked Kitaev chains and higher-order TSCs. For $P\bar{1}$ and $P4/m$ with the A_u representation, $\mathcal{X}^{\mathrm{WTSC}}$ coincides with the maximal $(\mathbb{Z}_2)^m$ subgroup of X^{BdG}. (For $P4/m$, $m = 2, 2, 7$ in one, two, and three dimensions.) For $P4/m$ with B_u and B_g representations, $\mathcal{X}^{\mathrm{WTSC}}$ is only a subgroup of the maximal $(\mathbb{Z}_2)^m$ subgroups of X^{BdG}, and we explain the correspondence in the Supplementary Materials.

DISCUSSION

We advanced the theory of SIs for TSCs and computed the indicator groups explicitly for all space groups and pairing symmetries. We showed that the refinement proposed in (*20*, *21*) enables the detection of a variety of phases, including both "first-order" (i.e., conventional) and higher-order TSCs. This is perhaps surprising, as the refinement only captures phases with zero-dimensional Majorana modes in the case of inversion symmetry studied in (*20*, *21*). Furthermore, we found that the same indicator could correspond to a possibly gapped or a necessarily gapless phase depending on the additional spatial symmetries that are present. Such observations should be contrasted with the familiar case of the Fu-Kane parity criterion for topological

Table 3. List of $\mathcal{X}^{\mathrm{WTSC}}$ for class DIII systems with $P\bar{1}$, P4, and $P4/m$ symmetry in each spatial dimension.

SG (rep of Δ_k)	1D	2D	3D
$P\bar{1}$ (A_u)	$\mathbb{Z}_2$	$(\mathbb{Z}_2)^3$	$(\mathbb{Z}_2)^7$
$P4$ (B)	$\mathbb{Z}_1$	$(\mathbb{Z}_2)^2$	$(\mathbb{Z}_2)^2$
$P4/m$ (A_u)	$(\mathbb{Z}_2)^2$	$(\mathbb{Z}_2)^2$	$(\mathbb{Z}_2)^7$
$P4/m$ (B_u)	$\mathbb{Z}_1$	$(\mathbb{Z}_2)^2$	$(\mathbb{Z}_2)^3$
$P4/m$ (B_g)	$\mathbb{Z}_1$	$\mathbb{Z}_2$	$\mathbb{Z}_2$

insulators (*30*), which is valid independent of the other spatial symmetries in the system. This suggests that caution must be used in diagnosing a TSC using only part of the spatial symmetries, and it is desirable to perform a more comprehensive analysis taking into account the entire space group preserved by the superconductor, as is done in the present work.

As a concrete example, our analysis for systems with C_4 rotation symmetry revealed a new $\mathbb{Z}_2$-valued index, which we denote by ν_{C_4}. We argued that $\nu_{C_4} = 1$ implies the system is a helical TSC when the system is gapped or indicates a gapless phase when inversion symmetry is present and the superconducting pairing has even parity. Within the weak pairing assumption, this nontrivial index can be realized in systems with *d*-wave pairing and an odd number of filled Kramers pairs in the normal state (section S4). When inversion symmetry is broken such that mixed-parity pairing becomes possible, one could gap out the nodes of the superconducting gap by increasing the *p*-wave component, and the end result will be a helical TSC. A similar picture was proposed in (*47*), although the role of the SI was not recognized there. Such mechanism may be possible for the (proximitized) superconductivity on the surfaces of 3D materials, where the surface termination breaks inversion symmetry and can give rise to Rashba spin-orbit coupling. If the system has C_4 rotational symmetry and a SC pairing with $\chi_{C_4} = -1$ (e.g, *D* wave) is realized in the bulk, the induced surface superconductor on a C_4-preserving surface will be topological when the number of filled surface-Kramers pair at the momenta Γ and *M* is odd in the normal state. The surface SC, if viewed as a stand-alone system, will be either a nodal or helical TSC.

Alternatively, one could also replace the innate surface state in the proposal above by an independent 2D system in which superconductivity is induced by proximity coupling to a *d*-wave superconductor.

More generally, it is interesting to ask how our theory could be applied to surface superconductivity, especially for the anomalous surface states arising from a topological bulk (*48*). Conceptually, one can also compute the refined SI of a nonsuperconducting insulator by assuming an arbitrarily weak pairing amplitude with a chosen pairing symmetry. If the insulator is atomic to begin with (i.e., its ground state is smoothly deformable to a product state of localized electrons), the refined SI is trivial by definition. However, if the insulator is topological, its refined SI may be nontrivial. As the pairing can be arbitrarily weak in the bulk, this nontrivial refined SI is a statement on the nature of the TSC realized at the surface. As a concrete example, consider an inversion-symmetric strong TI. If we assume an odd-parity pairing is added to the system, one sees that the refined SI will be nontrivial. This setup is formally realized for an S-TI-S junction with a π phase shift, and the helical Majorana mode that appears (*48*) is consistent with the refined SI discussed above. This correspondence between a strong TI and a (higher-order) TSC is quite general and has been noted earlier in (*49*) assuming C_4 symmetry. Given the vast majority of TI candidates discovered from materials database searches (*16*–*18*) are in fact (semi-)metallic, they may have superconducting instability and could realize a TSC based on the analysis above.

On a more technical note, we remark that our theory does not incorporate the Pfaffian invariant discussed in (*21*), although this invariant can be readily related to the number of filled states in the normal-state band structure within the weak-pairing assumption. While it will be interesting to incorporate it into our formalism, the Pfaffian invariant is different from the usual representation counts as it is $\mathbb{Z}_2$ valued. This will bring about some technical differences in the computation of the SI group, although a systematic computation is still possible (*21*).

Last, we note that in our analysis for the physical meaning of ν_{C_4} we introduced the notion of WTSCs, examples of which include the 1D Kitaev chain and 2D higher-order TSCs, as well as weak phases constructed by stacks of them. As a more nontrivial example, we note that the set of WTSCs also includes "first-order" examples like the even entries for the $\mathbb{Z}$-valued classification of class DIII superconductors in 3D. While we have developed a formalism for the partial diagnosis of such TSCs, our analysis does not result in a full classification for WTSCs. It will be interesting to explore how the full classification can be obtained, as well as the unique physical properties, if any, that are tied to the notion of WTSCs.

SUPPLEMENTARY MATERIALS

Supplementary material for this article is available at http://advances.sciencemag.org/cgi/content/full/6/18/eaaz8367/DC1

REFERENCES AND NOTES

1. M. R. Norman, The challenge of unconventional superconductivity. *Science* **332**, 196–200 (2011).
2. X.-L. Qi, S.-C. Zhang, Topological insulators and superconductors. *Rev. Mod. Phys.* **83**, 1057–1110 (2011).
3. Y. Ando, L. Fu, Topological crystalline insulators and topological superconductors: From concepts to materials. *Annu. Rev. Condens. Matter Phys.* **6**, 361–381 (2015).
4. M. Sato, Y. Ando, Topological superconductors: A review. *Rep. Prog. Phys.* **80**, 076501 (2017).
5. S. R. Elliott, M. Franz, Colloquium: Majorana fermions in nuclear, particle, and solid-state physics. *Rev. Mod. Phys.* **87**, 137–163 (2015).
6. D. S. Freed, G. W. Moore, Twisted equivariant matter. *Annales Henri Poincaré* **14**, 1927–2023 (2013).
7. H. Song, S.-J. Huang, L. Fu, M. Hermele, Topological phases protected by point group symmetry. *Phys. Rev. X* **7**, 011020 (2017).
8. J. Kruthoff, J. de Boer, J. van Wezel, C. L. Kane, R.-J. Slager, Topological classification of crystalline insulators through band structure combinatorics. *Phys. Rev. X* **7**, 041069 (2017).
9. R. Thorngren, D. V. Else, Gauging spatial symmetries and the classification of topological crystalline phases. *Phys. Rev. X* **8**, 011040 (2018).
10. S.-J. Huang, H. Song, Y.-P. Huang, M. Hermele, Building crystalline topological phases from lower-dimensional states. *Phys. Rev. B* **96**, 205106 (2017).
11. E. Khalaf, H. C. Po, A. Vishwanath, H. Watanabe, Symmetry indicators and anomalous surface states of topological crystalline insulators. *Phys. Rev. X* **8**, 031070 (2018).
12. K. Shiozaki, M. Sato, K. Gomi, Atiyah-Hirzebruch spectral sequence in band topology: general formalism and topological invariants for 230 space groups. arXiv:1802.06694 (2018).
13. Z. Song, S.-J. Huang, Y. Qi, C. Fang, M. Hermele, Topological states from topological crystals. arXiv:1810.02330 (2018).
14. H. C. Po, A. Vishwanath, H. Watanabe, Symmetry-based indicators of band topology in the 230 space groups. *Nat. Commun.* **8**, 50 (2017).
15. B. Bradlyn, L. Elcoro, J. Cano, M. G. Vergniory, Z. Wang, C. Felser, M. I. Aroyo, B. A. Bernevig, Topological quantum chemistry. *Nature* **547**, 298–305 (2017).
16. T. Zhang, Y. Jiang, Z. Song, H. Huang, Y. He, Z. Fang, H. Weng, C. Fang, Catalogue of topological electronic materials. *Nature* **566**, 475–479 (2019).
17. M. G. Vergniory, L. Elcoro, C. Felser, N. Regnault, B. A. Bernevig, Z. Wang, A complete catalogue of high-quality topological materials. *Nature* **566**, 480–485 (2019).
18. F. Tang, H. C. Po, A. Vishwanath, X. Wan, Comprehensive search for topological materials using symmetry indicators. *Nature* **566**, 486–489 (2019).
19. S. Ono, Y. Yanase, H. Watanabe, Symmetry indicators for topological superconductors. *Phys. Rev. Res.* **1**, 013012 (2019).
20. A. Skurativska, T. Neupert, M. H. Fischer, Atomic limit and inversion-symmetry indicators for topological superconductors. arXiv:1906.11267 (2019).
21. K. Shiozaki, Variants of the symmetry-based indicator. arXiv:1907.13632 (2019).
22. J. Langbehn, Y. Peng, L. Trifunovic, F. von Oppen, P. W. Brouwer, Reflection-symmetric second-order topological insulators and superconductors. *Phys. Rev. Lett.* **119**, 246401 (2017).
23. E. Khalaf, Higher-order topological insulators and superconductors protected by inversion symmetry. *Phys. Rev. B* **97**, 205136 (2018).
24. X.-L. Qi, T. L. Hughes, S.-C. Zhang, Topological invariants for the Fermi surface of a time-reversal-invariant superconductor. *Phys. Rev. B* **81**, 134508 (2010).

25. Y. Wang, M. Lin, T. L. Hughes, Weak-pairing higher order topological superconductors. *Phys. Rev. B* **98**, 165144 (2018).
26. Y.-T. Hsu, W. S. Cole, R.-X. Zhang, J. D. Sau, Inversion-protected higher order topological superconductivity in monolayer WTe_2. arXiv:1904.06361 (2019).
27. J. Ahn, B.-J. Yang, Higher-order topological superconductivity of spin-polarized fermions. arXiv:1906.02709 (2019).
28. L. Fu, E. Berg, Odd-parity topological superconductors: Theory and application to $Cu_xBi_2Se_3$. *Phys. Rev. Lett.* **105**, 097001 (2010).
29. M. Sato, Topological odd-parity superconductors. *Phys. Rev. B* **81**, 220504 (2010).
30. L. Fu, C. L. Kane, Topological insulators with inversion symmetry. *Phys. Rev. B* **76**, 045302 (2007).
31. A. P. Schnyder, S. Ryu, A. Furusaki, A. W. W. Ludwig, Classification of topological insulators and superconductors in three spatial dimensions. *Phys. Rev. B* **78**, 195125 (2008).
32. M. Sato, S. Fujimoto, Majorana fermions and topology in superconductors. *J. Physical Soc. Japan* **85**, 072001 (2016).
33. H. C. Po, H. Watanabe, A. Vishwanath, Fragile topology and wannier obstructions. *Phys. Rev. Lett.* **121**, 126402 (2018).
34. B. Bradlyn, Z. Wang, J. Cano, B. A. Bernevig, Disconnected elementary band representations, fragile topology, and Wilson loops as topological indices: An example on the triangular lattice. *Phys. Rev. B* **99**, 045140 (2019).
35. A. Y. Kitaev, Unpaired majorana fermions in quantum wires. *Physics-Uspekhi* **44**, 131–136 (2001).
36. S. Ono, H. Watanabe, Unified understanding of symmetry indicators for all internal symmetry classes. *Phys. Rev. B* **98**, 115150 (2018).
37. C. J. Bradley, A. P. Cracknell, in *The Mathematical Theory of Symmetry in Solids* (Oxford Univ. Press, 1972).
38. Z. Song, T. Zhang, Z. Fang, C. Fang, Quantitative mappings between symmetry and topology in solids. *Nat. Commun.* **9**, 3530 (2018).
39. M. I. Aroyo, D. Orobengoa, G. de la Flor, E. S. Tasci, J. M. Perez-Mato, H. Wondratschek, Brillouin-zone database on the *Bilbao Crystallographic Server*. *Acta Crystallogr. A* **70**, 126–137 (2014).
40. C. Fang, M. J. Gilbert, B. A. Bernevig, Bulk topological invariants in noninteracting point group symmetric insulators. *Phys. Rev. B* **86**, 115112 (2012).
41. C.-K. Chiu, H. Yao, S. Ryu, Classification of topological insulators and superconductors in the presence of reflection symmetry. *Phys. Rev. B* **88**, 075142 (2013).
42. M. Sato, Y. Tanaka, K. Yada, T. Yokoyama, Topology of Andreev bound states with flat dispersion. *Phys. Rev. B* **83**, 224511 (2011).
43. L. Fu, Odd-parity topological superconductor with nematic order: Application to $Cu_xBi_2Se_3$. *Phys. Rev. B* **90**, 100509 (2014).
44. S. Yonezawa, Nematic superconductivity in doped Bi_2Se_3 topological superconductors. *Condens. Matter* **4**, 2 (2019).
45. S. A. Yang, H. Pan, F. Zhang, Dirac and Weyl superconductors in three dimensions. *Phys. Rev. Lett.* **113**, 046401 (2014).
46. D. V. Else, H. C. Po, H. Watanabe, Fragile topological phases in interacting systems. *Phys. Rev. B* **99**, 125122 (2019).
47. Y. Tada, N. Kawakami, S. Fujimoto, Pairing state at an interface of Sr_2RuO_4: Parity-mixing, restored time-reversal symmetry and topological superconductivity. *New J. Phys.* **11**, 055070 (2009).
48. L. Fu, C. L. Kane, Superconducting proximity effect and majorana fermions at the surface of a topological insulator. *Phys. Rev. Lett.* **100**, 096407 (2008).
49. N. Bultinck, B. A. Bernevig, M. P. Zaletel, Three-dimensional superconductors with hybrid higher-order topology. *Phys. Rev. B* **99**, 125149 (2019).

Acknowledgments: We would like to thank E. Khalaf, T. Morimoto, K. Shiozaki, A. Vishwanath, Y. Yanase, and M. Zaletel for discussions and collaborations on related topics. **Funding:** The work of S.O. is supported by the Materials Education program for the future leaders in Research, Industry, and Technology (MERIT). The work of H.C.P. is supported by a Pappalardo Fellowship at MIT and a Croucher Foundation Fellowship. The work of H.W. is supported by JSPS KAKENHI grant no. JP17K17678 and by JST PRESTO grant no. JPMJPR18LA. **Author contributions:** All authors designed the research, performed the research, contributed new reagents/analytic tools, analyzed the data, and wrote the manuscript. **Competing interests:** The authors declare that they have no competing interests. **Data and materials availability:** All data needed to evaluate the conclusions in the paper are present in the paper and/or the Supplementary Materials. Additional data related to this paper may be requested from the authors.

Submitted 12 October 2019
Accepted 5 February 2020
Published 1 May 2020
10.1126/sciadv.aaz8367

Citation: S. Ono, H. C. Po, H. Watanabe, Refined symmetry indicators for topological superconductors in all space groups. *Sci. Adv.* **6**, eaaz8367 (2020).